Survival, growth and gene expression in zebrafish (*Danio rerio*) larvae exposed to silver nanoparticles

Marthe Røgeberg

Master thesis in Toxicology

Department of Biology

UNIVERSITETET I OSLO

September 2011

Acknowledgement

The work in this thesis was carried out at CRRT, Norwegian School of Veterinary Science (NVH). The thesis was part of the NanEAU project and is a collaboration between NVH and CRP - Gabriel Lippmann institute. NanEAU is supported by Fonds National de la Recherche Luxembourg within the “Core2008” program (C08/SR/07).

First of all I want to thank my supervisor at NVH, Professor Erik Ropstad for always being available, for comments on my writing and for motivating talks and discussions. I want to thank Dr. Arno C. Gutleb (CRP – Gabriel Lippmann institute) for introducing me to nano research and quick replies. I would also like to thank my internal supervisor at the University of Oslo, Professor Ketil Hylland for supervision and for giving me the opportunity to participate in research activities outside my thesis and course work.

I would like to thank Maurizo Gault and Wiggo Sandberg (FHI) for teaching me about nanoparticle suspensions, Tore-Geir Iversen at Radiumhospitalet for giving access to and guidance on characterization of nanoparticles using DLS and Lene Hermansen (NVH) for preparation of grids and guidance on operating the TEM. I want to thank the staff at the AZlab, especially facility manager Jan Roger Torp with his great knowledge about the zebrafish and zebrafish husbandry, his patience and many advices.

Special thanks go to Camilla Karlsson, for your great help, good spirits, for excellent supervision in the fish lab, with the microarrays, qPCR and data analyses. To Nina Hårdnes for your help in the fish lab and with the sampling procedures, and Dr. Steven Verhaegen at NVH for helping me getting my head around the Ingenuity Pathway Analyses.

Finally, I want to thank my fellow students, friends, my boyfriend Thomas and my family for believing in me, your encouragement and good times.

Abstract

The objective of this thesis was to evaluate the toxicity of silver nanoparticles at predicted environmentally relevant concentrations (i.e. 0.01, 0.1, 0.5 and 1.0 mg/L by mass of nanoparticles). One concentration of silver nitrate (0.01 mg/L) was included to compare the effects of silver ions (from $AgNO_3$) with effects of the same concentration of nanoparticles. Zebrafish (*Danio rerio*) larvae were exposed in a critical window of larval development (i.e. 6 dpf – 21 dpf) to quantify effects on survival, growth and changes in gene expression.

Suspended nanoparticles were found to be polydispersed and there was a tendency towards broader size distributions and bigger agglomerates with increasing concentration. No negative effects were observed in survival or growth. However, exposure to the highest concentration of silver nanoparticles (0.01 mg/L) resulted in a significant positive effect on survival. Microbiological analysis of water samples from the exposure tanks showed that there were more microorganisms in the sample collected from the highest exposure concentration, indicating that increased survival was most likely not explained by antibacterial properties of silver nanoparticles. Changes in gene expression following exposure to equal concentrations of silver nanoparticles and silver nitrate (i.e. 0.01 mg/L) resulted in distinctive gene expression profiles, with silver nanoparticles inducing changes in a much higher number of genes than silver nitrate. Both gene expression profiles appear to associate with the visual system and cardiovascular health. Silver nanoparticles induce changes in several genes involved in the negative feedback-loop of the circadian rhythm system and pathways associated with the activation of nuclear receptors.

Index

Abbreviations

A	Average expression
Ag	Silver
Ag^+	Silver cation
Cl^-	Chloride
$AgNO_3$	Silver nitrate
AAALAC	Association for Assessment and Accreditation of Laboratory Animal Care International
ANOVA	Analysis of variance
Artemia	Brine shrimp
AZlab	Aleström Zebrafish lab
BA	Blood agar
cDNA	Complementary DNA
Chlamydomonas reinhardtii	Green algae
cRNA	Complementary RNA
C_T	Cycle threshold
CTP	Cytidine triphosphate
Cyprius carpio	Carp
Cy3	Cyanine-3
Cy5	Cyanine-5
Danio rerio	Zebrafish
DLS	Dynamic light scattering
DNA	Deoxyribonucleic acid
DNase	Deoxyribonuclease
Dpf	Days post fertilization
Drosophila	Fruit fly

E	Amplification efficiencies
GAL	Gene pix array list
GH	General hardness
HCl	Hydrochloric acid
IPA	Ingenuity Pathway Analysis
Kcps	Kilo-counts per seconds
KH	Carbonate hardness
limmaGUI	Linear models for microarrays graphical user interface
Lymnae stagnalis	Freshwater snail
L929	Mouse fibroblast cells
M	Fold change ratio
mRNA	Messenger RNA
NaOH	Sodium hydroxide
Neris diversicolor	Polychaete
NVH	Norwegian school of veterinary science
PCA	Plate count agar
TEM	Transmission electron microscopy
NH_3	Ammonia
NH_4^+	Ammonium
NO_2^-	Nitrite
NO_3^-	Nitrate
OECD	The Organization for Economic Co-operation and Development
Oryzias latipes	Japanese medaka
PC12	Rat neuroendocrine cells
PDI	Polydispersity index
PECs	Predicted environmental concentrations
qPCR	Real-time quantitative polymerase chain reaction

RNA	Ribonucleic acid
RNase	Ribonuclease
ROS	Reactive Oxygen Species
Rpm	Revolutions per minute
SE	Standard error
Z.avg	Mean hydrodynamic diameter

1. Introduction

Nanoparticles are commonly defined as particles with at least one dimension between 1 and 100 nm. It is the inverse relationship between particle size and reactivity that provides nanoparticles with the unique mechanical, electrical and optical properties, which are exploited in many applications of nanotechnology (Donaldson et al. 2004; Oberdörster et al. 2005).

1.1 Nanosilver

Silver nanoparticles are one of the most common types of nanoparticles in use and were chosen for this study because of their wide area of application and that they are known to induce toxicity in a variety of cells types (Farkas et al. 2010; Morones et al. 2005; Skebo et al. 2007). Their wide range of application is mainly due to their antibacterial properties. Nanosilver can be found in a variety of commercially available products such as technical textiles, cosmetics, refrigerators, food packing, washing machines etc (Wijnhoven et al. 2009). Analyses of effluents from a washing machine containing nanosilver

With the increased production volume and use of nanotechnology-based products comes the concern about the toxicity that might be triggered by unintentionally or deliberately exposure to silver nanoparticles (Balbus et al. 2007; Chaloupka et al. 2010; Faunce & Watal 2010). Exposure models based on current knowledge and production volume have estimated predicted environmental concentrations (PECs) of nanoparticles in different compartments to be in the low range (mg/kg or ng/L) (Gottschalk et al. 2009; Mueller & Nowack 2008). It has just recently been demonstrated that several aquatic organisms accumulate silver nanoparticles when exposed to concentrations in the low range predicted to occur in water (Cong et al. 2011; Croteau et al. 2011; Gaiser et al. 2009), which raises concern about the possible impacts.

It is well known from studies of ultrafine particles that deposition in the respiratory system and toxicity are dependent on the particle size and surface area (Oberdörster 2000). Particles deposited in the alveolar region may be phagocytosed by alveolar macrophages and cleared from the lungs via the mucociliary escalator. Activation of macrophages may trigger

pathological damage in the lung through the release of pro-inflammatory cytokines and formation of reactive oxygen species (ROS) (Maynard & Kuempel 2005).

Assessments of pulmonary uptake have shown that inhaled nanoparticles, including agglomerates, appear to be phagocytosed by alveolar macrophages in rats and mice (Stebounova et al. 2011; Takenaka et al. 2001). Silver nanoparticles have also been observed to redistribute from the lungs and after oral administration, into the systemic circulation and reappear in various organs, such as the liver, kidney, spleen, brain, heart and testis of mice and rats (Park et al. 2010a; Takenaka et al. 2001).

A large proportion of inhaled nanoparticles have been found to deposit in the nasal cavity of rodents (Takenaka et al. 2001). Particles deposited in the nasal region have previously been found to be transported to the olfactory bulb via olfactory nerves and raises concern about the ability of nanoparticles to induce neurotoxic effects (Oberdörster et al. 2004).

Nanosilver have been demonstrated to possess a higher capability to cross the blood-brain barrier in rats via subcutaneous injection relative to silver particles in the micro size (Tang et al. 2008). Further, *in vitro* studies conducted with rat neuroendocrine cells (PC-12) have found silver nanoparticles to be internalized and to be potent in inducing proinflammatory responses and cytotoxicity in rat neuroblast and microvessel endothelial cells (Schrand et al. 2008; Skebo et al. 2007; Trickler et al. 2010).

In vitro assays have demonstrated that nanoparticles are capable of being taken up in a variety of cell types and to accumulate in cellular compartments, such as the nucleus and mitochondria (Asharani et al. 2009; Asharani et al. 2008; Choi et al. 2010; Mahmood et al. 2010). There is substantial evidence that silver nanoparticles induce cytotoxic and genotoxic effects *in vitro*, through mechanisms interfering with mitochondrial function, membrane integrity, formation of reactive oxygen species (ROS), DNA damage and cell death (Arora et al. 2008; Asharani et al. 2009; Braydich-Stolle et al. 2005; Farkas et al. 2010; Foldbjerg et al. 2011; Hsin et al. 2008; Hussain et al. 2005; Park et al. 2010b; Schrand et al. 2008).

Further, it has been demonstrated that silver nanoparticles give rise to significant DNA damage in cells in a dose-dependent manner (Asharani et al. 2009) and that nanoparticles induce apoptosis more significantly in mouse fibroblast cells (L929) than silver nanoparticles in the micro-size (Wei et al. 2010).

There is controversy whether the observed toxicity is induced by the nanoparticles itself or through the dissolution and release of silver ions (Ag^+). Nanoparticles have also been suggested to induce toxicity by releasing ions at the target site (Choi et al. 2010). The effects of silver nanoparticles are often compared to that induced by free ions after exposure to silver nitrate ($AgNO_3$), which functions as an ion source. When comparing toxicity of silver nanoparticles and $AgNO_3$ to photosynthesis of green algae (*Chlamydomonas reinhardtii*) as a function of Ag^+ in the original suspensions it seems that nanoparticles induce a much higher toxicity, which cannot solemnly be explained by the original Ag^+ (Navarro et al 2008). Silver ions and nanoparticles have been found to result in distinct responses in the gene expression in both medaka (*Oryzias latipes*) and zebrafish and indicate that they work through different mechanisms (Chae et al. 2009; Griffitt et al. 2009). Studies comparing the effects on survival at an early life stage of several fish species have discovered nanoparticles to be more toxic than silver nitrate indicated by a lower survival in embryos exposed to nanoparticles (Chae et al. 2009; Laban et al. 2010). These results are in contrast to another reporting indicating that that Ag^+ caused lower survival than silver nanoparticles (Yeo & Yoon 2009). Comparisons of metal burden measured in gills of adult zebrafish exposed *in vivo* found that silver nanoparticles caused higher silver burden than silver ions (Griffitt et al. 2009), whilst more silver was found to accumulate in primary cells of gill epithelia cultured *in vitro* and exposed to silver nitrate compared to the same concentration of silver nanoparticles (Farkas et al. 2011a).

1.2 Size, size distribution and state of agglomeration

The behavior and fate of nanoparticles in biological systems is attributed to the stability of the particles in relevant media, which may be affected by a variety of environmental and biological factors (ionic strength, temperature, organic material, biological processes etc.), in addition to the particles shape, surface chemistry, surface area and state of agglomeration (Cumberland & Lead 2009; Fubini et al. 2010; Liu et al. 2011). The attractive forces between nanoparticles in suspension increase inversely with particle size and it has been demonstrated to be nearly impossible to avoid agglomeration of nanoparticles when introduced into test systems (Brain et al. 2009; Powers et al. 2007; Römer et al. 2011). Agglomeration shifts the size distribution to higher sizes and may alter the toxicological

properties of the primary particles under study (Balbus et al. 2007; Dhawan et al. 2009; Fubini et al. 2010).

There are various strategies available to increase the stability and dispersion of nanoparticles in toxicological studies. Addition of sound energy (by an ultrasonicator) agitate nanoparticles in suspension and may increase dispersion in the sample (Dhawan et al. 2009; Laban et al. 2010), or one can mitigate surface reactivity by coating with polymers or suspend the particles in stabilizing agents (Dhawan et al. 2009; Skebo et al. 2007).

To be able to investigate the significance of size in toxicological studies it is necessary to characterize the size, size distribution and agglomeration of nanoparticles in relevant medium (Balbus et al. 2007; Dhawan et al. 2009; Powers et al. 2007). Available methods for characterization of size and state of agglomeration (e.g. optical spectroscopy, dynamic light scattering, transmission or scanning electron microscopy) are based on various physiochemical principles, and because the different methods often are inconclusive, it is recommended to apply more than one method for the characterization (Dhawan et al. 2009; Jones & Grainger 2009; Powers et al. 2007). In this study, there were applied two methods for characterization, i.e. dynamic light scattering (DLS) and transmission electron microscopy (TEM).

DLS can be applied for quantitative assessments of the hydrodynamic diameters of nanoparticles in suspension. A colloid dispersion is illuminated with laser and the time-dependent fluctuations in the intensity of scattered light is analyzed and used for calculations of the hydrodynamic diameter of the particles (performed by the instrument software) (Kaszuba et al. 2008). The hydrodynamic diameter is related to the diffusion coefficient of molecules undergoing Brownian motion and is the diameter of a sphere that has the same translational diffusion coefficient as the particle being measured (Kaszuba et al. 2008). Sizes measured by DLS are intensity-weighted sizes, which mean that the size distributions are a plot of the relative intensity of light scattered by particles in various size classes. The output reports the mean hydrodynamic diameter and estimated width of distribution (polydispersity index). Reported average count rate (number of photons detected per second) can be used for evaluating sample quality. Increased count rates indicate agglomerating samples, while lower count rates indicate sedimenting or dissolving samples.

A common method used for assessments of metallic nanoparticles in toxicological studies is the imaging of dehydrated samples of stock or test solutions by TEM (Jones & Grainger 2009). Analyses of nanoparticles based on TEM images can be used for both quantitative assessment of size and size distribution by examination of sufficient particles to provide statistically valid results, and qualitative assessment of particle morphology, size distribution and state of agglomeration in the samples under investigation (Powers et al. 2007; Tiede et al. 2008).

1.3 The zebrafish model in toxicological assessments

In vitro assays are simplified models designed for assessments of cellular uptake and toxicity (Jones & Grainger 2009) and have been demonstrated to be of limited value for predicting the toxicological outcome of nanoparticle toxicity *in vivo* (Sayes et al. 2009). Zebrafish is a tropical freshwater fish of the Cyprinid family originating from South-Asia, which is a popular vertebrate model species in biological research and used for toxicological screening of new chemicals, including assessments in nanotoxicology (Fako & Furgeson 2009; Hill et al. 2005). Zebrafish has been used in biological research since the 1930s and there is extensive information on its development, physiology and biochemistry. The sequencing of the zebrafish genome was initiated by the Wellcome Trust Sanger Institute (Hinxton, UK) in 2001 and is now near completed (http://www.sanger.ac.uk/Projects/D_rerio/). The zebrafish genome appears to be highly homogeneous to the mammalian, which makes studies of toxicological endpoints in zebrafish useful for prediction of toxicity in both aquatic organisms and mammals (Aleström et al. 2006; Hill et al. 2005; Zhang et al. 2003).

The small size, robustness, reproductive capacity and short generation time makes it relative easy and inexpensive to maintain zebrafish under experimental conditions. Adult fish grow to about 5-6 cm in length and have the capacity to produce 200-300 eggs per spawning if handled under appropriate conditions. The developing embryo is transparent and surrounded by a chorion until hatching occurs 2-3 days post fertilization (dpf), when most of its morphogenesis is completed. Hatched larvae are raised in small containers (1-2 L) under semi-static conditions, which require daily replacement of at least 1/3 of the water in the containers until they are big enough to be transferred to bigger tanks connected to a flow-through system (Westerfield 2000).

Foraging starts after the yolk is depleted around 4-6 dpf, followed by a critical period of extensive growth and subsequent natural drop in survival dependent on the foraging success (Kimmel et al. 1995). This time period from around 6 dpf – 21 dpf has been observed to be a sensitive window for assessing toxic effects of contaminants in fish (Andersen et al. 2003; Bourrachot et al. 2008; Powers et al. 2010). An advantage with exposing zebrafish larvae in this period is that they are not dependent on a flow-through system and one avoids the risk for contaminating the laboratory circulating system with the test substance.

Several manufacturers have constructed microarrays of zebrafish complementary DNA or oligonucleotides, enabling genome wide transcription profiling of effects following exposure to a toxicant, proved to be promising in the search for relevant biomarkers and endpoints for toxicity (Nel et al. 2006).

Microarrays consists of a number of probes made of known oligonucleotides (or complementary DNA), which is printed in a matrix on a solid slide and allows the analysis of several thousands genes simultaneously. Changes in the gene expression (fold change) induced by exposure to toxicants can be examined by quantification of intensity ratios of red and green fluorescence that arise from the hybridization of reverse transcribed messenger RNA (mRNA) isolated from exposed samples relative to the levels in the unexposed (Nuber 2005). The quality of the data generated by microarrays is dependent on both biological and technical variations, which may be avoided by good experimental design and through the processing and normalization of the generated data (White & Salamonsen 2005).

Normalization of the fluorescence intensities within arrays (print-tip group locally weighted scatterplot smoothing) and between arrays (scale) is crucial to eliminate technical variations in the dataset (Smyth & Speed 2003; Wettenhall & Smyth 2004) and can be performed in the limmaGUI (linear models for microarrays Graphical User Interface) package produced for Bioconductor's R.

A RNA Target file with information about the microarray hybridizations, slide numbers and corresponding output file from the image analyses is uploaded to the limmaGUI package together with a Gene Pix Array List (GAL) provided by manufacturer of the arrays, which describes the size and position of the blocks, the layout of feature-indicators and the names and identifiers of the printed substances associated with each feature-indicator. A Spot Type

file with information about the color codes and names is optional but and can be uploaded to limmaGUI to distinguish between genes, controls and blanks.

The limmaGUI package fits a linear model to the data, tests the hypothesis that the expression values of the genes in the exposed groups is equal to the expressions in the unexposed and adjusts the p-values for multiple testing (Smyth 2004; Wettenhall & Smyth 2004). The adjustment is based on the Benjamini and Hockberg method, which control the false discovery rate – a challenge with analysis of large data sets, and means that the expected proportion of false positives in the selection is controlled to be less than the threshold selected for the analysis, i.e. less than 5 % for a threshold of 0.05 (Smyth 2005).

MA scatter plots with ($\log_2$) fold change ratios (M) plotted against the average expression (A) are known to be convenient for visualization of the distribution of induced or repressed genes, and assessment of the quality of the microarray data based on the shape of the scatter plot (White & Salamonsen 2005). The data are considered of good quality if the spots are distributed as an elongated comet around M=0 (White & Salamonsen 2005).

It is common to analyze a set of genes from the microarray result by real-time quantitative polymerase chain reaction (qPCR) in order to validate the fold changes quantified by the microarrays (Denslow et al. 2007; Morey et al. 2006). This technique requires appropriate primers pairs (forward and reverse) to be designed, to be able to amplify the relevant target genes. The SYBR Green assay applied for the qPCR in the present study incorporates a fluorescence dye, and the number of amplifying cycles required to generate sufficient fluorescence (the cycle threshold) reflects the abundance of the target in the sample.

C_T values need to be normalized to the expression of a gene, which is equally expressed (not affected by the exposure) in the samples from both the exposed and unexposed (Tang et al). Normalized C_T values are analyzed by the Livak method (Livak & Schmittgen 2001) to determine the mean fold change of the target genes in the exposed samples relative to the fold change in the unexposed.

Ingenuity Pathway Analysis (IPA, http://www.ingenuity.com) is useful for assessments of molecular pathways, canonical pathways (typical pathways known to be associated with expression of the identified genes), biological functions and diseases that are most significantly associated with the differently expressed genes detected by microarrays.

Uploaded gene identifiers (IDs) are uploaded to the online java-based software, which maps the IDs to mammalian homologues and corresponding information stored in the Ingenuity Knowledge Base. The output from IPA is based on the ratios of the number of molecules from the uploaded dataset that map to each pathway, divided by the total of molecules identified to be involved in the same pathway. Assigned p-values (calculated by the right-tailed Fisher's exact test) determine the probability that the association between genes in the uploaded dataset and pathways or biological functions are due to chance alone or can be explained by the parameters under investigation.

1.4 Objective of study

With the considerable increase in production volume and widespread use of engineered silver nanoparticles there is a growing concern about the potential risk associated with nanotoxicology.

The overall objective of this study was to evaluate the toxicity of silver nanoparticles at environmentally relevant concentrations during early life development using zebrafish as a model organism.

Zebrafish was chosen as test species to examine the toxicity of silver nanoparticles on both the phenotypic and molecular level, and because zebrafish can serve as a model species for assessment of the toxicity induced in other vertebrates.

To evaluate the toxicity of silver nanoparticles at predicted environmentally relevant concentrations we exposed zebrafish to a range of low concentrations (by mass of silver nanoparticles) and one concentration of $AgNO_3$ to:

- Characterize the size and size distribution of nanoparticles suspended in exposure solutions of different concentrations.
- Quantify effects on changes in survival in a critical window of larval development
- Quantify effects on growth based on body length on 21 dpf
- Clarify and compare changes in gene expression following exposure to a low concentration of silver nanoparticles and the same concentration of $AgNO_3$.

- Validate the microarray results by qPCR
- Clarify if the amount of microorganisms in fish tank water could explain differences in survival.

2. Materials and methods

2.1 Nanoparticles and silver ion source

Silver (Ag) nanoparticles from PlasmaChem GmbH (Berlin, Germany) were provided as dry powder by the NanEAU project. The nominal size was specified to be 20 nm by the manufacturer. Silver nitrate ($AgNO_3$, CAS-no.: 7761-88-8) was applied as a silver ion source and was purchased from Sigma-Aldrich AS, Schnelldorf, Germany. Both particles and reagent were stored at room temperature away from light until required.

Fresh stock solutions with nominal concentrations of 1000 mg/L by mass of nanoparticles or silver nitrate powders were made every third day during the exposure period and stored at room temperature in a dark cabinet when not in use.

Silver nanoparticles (13 mg) and silver nitrate (13 mg) were weighed out in 50 mL-Falcon tubes on a milligram scaled weight. Autoclaved ultrapure water (11 mL) (Simplicity UV water purification system, Millipore Molsheim, France) was added to each tube before the powders were resuspended. Nanoparticle suspensions were mixed on a Labinco L46 vortexer and sonicated on ice with an UP200S ultrasonic processor (Hielscher Ultrasound, GmbH) for 3 min until 420 J of total energy was supplied to the solutions. Conditioned water from the zebrafish lab (2 mL) was added to the stock solutions to achieve a stock concentration of 1000 mg/L by mass of nanoparticles or reagent powder. Conditioned water (0.8 L) was added to each tank and spiked (Table 1) with stock solutions of silver nanoparticles or $AgNO_3$ to achieve nominal concentrations of 0.01, 0.1, 0.5 and 1.0 mg/L by mass of nanoparticle or reagent powder.

Table1. Amount of stock solution used to spike the conditioned water to appropriate concentrations. Stock solutions (1000 mg/L) were diluted in 0.4 L conditioned water at 50 % water change and 0.8 L conditioned water at 100 % water change. Conditioned water contained methylene blue.

Experimental group	50 % water change	100 % water change
Control	0.4 L conditioned water	0.8 L conditioned water
$AgNO_3$ 0.01 mg/L	4 µL stock	8 µL stock
Ag nano 0.01 mg/L	4 µL stock	8 µL stock
Ag nano 0.1 mg/L	40 µL stock	80 µL stock
Ag nano 0.5 mg/L	200 µL stock	400 µL stock
Ag nano 1.0 mg/L	400 µL stock	800 µL stock

Experimental tanks were filled with respective concentrations and drained before the exposure solutions and larvae were added and prior to renewal of tanks in order to minimize reduction of the nominal concentrations through adhesion of the test particles or reagent to the plastic tanks (Scown et al. 2010).

2.2 Characterization

Characterization of the nanoparticles suspended in the test media were performed by DLS, using a Zetasizer Nano Series instrument (Malvern instrument) and was performed at Radiumhospitalet on the fourth day in the exposure period (9 dpf). Samples from one replicate tank from each of the nanosilver groups, the control group and a sample of conditioned water were collected with disposable pipettes (VWR International, Oslo, Norway) and transferred to respective Eppendorf tubes.

At Radiumhospitalet each sample (100 µL) were transferred to transparent disposable cuvettes (Malvern, UV-cuvette micro). Mean hydrodynamic diameter (Z.avg), size distributions and polydispersity index (PDI) values were characterized by DLS, at 25±1°C and scattering angel of 173°.

There were collected samples from the exposure tanks for characterization by TEM on the same day as for the DLS characterizations (9 dpf). One droplet (~ 20 µL) from each sample was applied on carbon coated formvar copper grids (100 meshes) and excess fluid was dried by careful blotting with a filter paper as described by Bar-Ilan et al., 2009. Stock solution prepared for TEM assessments were allowed to attach for 10-15 min on the copper grid without blotting, as the assessments of the blotted samples appeared to result in few particles on the grid.

Samples were investigated by a Philips EM208S transmission electron microscope at 80 kV, the intensity adjusted to ~ 50% (± 1.0%) before the iTEM 5.0 software (Olympus Soft Imaging Solutions GmbH, Münster, Germany) was used to generate two-dimensional images of the nanoparticles in the dehydrated sample.

2.3 Test organisms and experimental design

Fish husbandry and exposure were carried out in the Aleström Zebrafish Lab (AZlab) at the Department of Basic Sciences and Aquatic Medicine, Norwegian School of Veterinary Science (NVH), Oslo, Norway.The Aleström zebrafish lab follows general guidelines for zebrafish care and husbandry and have since 1st of July 2008 been accredited by the Association for Assessment and Accreditation of Laboratory Animal Care International (AAALAC).

Adult AB wild type zebrafish (in house stock of the AZlab and adult AB wild type fish purchased from the Zebrafish International Resource Centre, Eugene, OR, USA) were bred to obtain sufficient number of larvae for the experiment. Two males and two females were placed in breeding tanks (2 L) and left over night. The genders were separated by a transparent barrier in each tank, resulting in a total of 32 tanks. Barriers were removed the next morning when lights were switched on and the fish were left alone to spawn for 2- 4 h. Eggs were collected from the bottom of each tank after 2 h and 4 h by pouring the tank water through a sieve. Collected eggs were rinsed with autoclaved conditioned water before they were transferred to petri dishes (90 mm, VWR International, Oslo, Norway) containing fresh autoclaved conditioned water.

Dead embryos were removed daily and the number of viable embryos were registered and evenly distributed in petri dishes, resulting in <100 embryos in each petri dish. Embryos/larvae in respective petri dishes were incubated in 28°C from the day of fertilization (0 dpf) until 5 dpf. Viable embryos/larvae were registered on a daily basis and dead individuals were removed.

Bleaching of embryos ~ 24 h post fertilization is a standard operating procedure at the AZlab and recommended in the Zebrafish Book (Westerfield 2000) to avoid contamination and spread of infection.

Approximately 24 h post fertilization the respective beakers (1 L) were filled with acquired solutions for the bleaching procedure Dead embryos were removed before each batch (< 100 individuals) of healthy embryos were transferred to a filter and the procedure carried out by periodically swirling of the filter in each beaker with fresh solutions adjusted to pH 7.0-7.5 by adding drops of HCl (1M) or NaOH (1M).

The procedure started with 5 min in bleach solution (85 % sodium hypochlorite and autoclaved conditioned water, pH 7.0), followed by 1 min in a second beaker containing sodiumthiosulfate (pH 7.0) and rinsed twice for 1 min each in two beakers containing rinse solution (autoclaved conditioned water, pH 7.5). After bleaching the number of viable embryos was counted and equal numbers of individuals were randomly distributed to new petri dishes (<100 embryos per 90 mm-petri dish).

There was a problem with fungal growth and an increased mortality rate in the first experimental set up. To avoid the problem of fungal growth a decision was made to add a 0.05% methylene blue stock solution (500 µL) to the conditioned water (1 L) used for the exposure on 7 dpf, resulting in a final concentration of 0.25 mg/L. This is a standard operating procedure at the AZlab during larvae husbandry and commercially available aquarium product.

On 5 dpf an equal number of larvae were transferred to each exposure tank (1 L), resulting in 52 individuals in each replicate tank and left alone to acclimate until the exposure start on 6 dpf. One exposure group consisted of 5 replicate tanks and there were six exposure groups in total (n=5). Five groups were exposed to silver nanoparticles (e.g. 0.01, 0.1, 0.5 and 1 mg/L), one group to silver nitrate (0.01 mg/L) and there was included one control group with conditioned water and methylene blue.

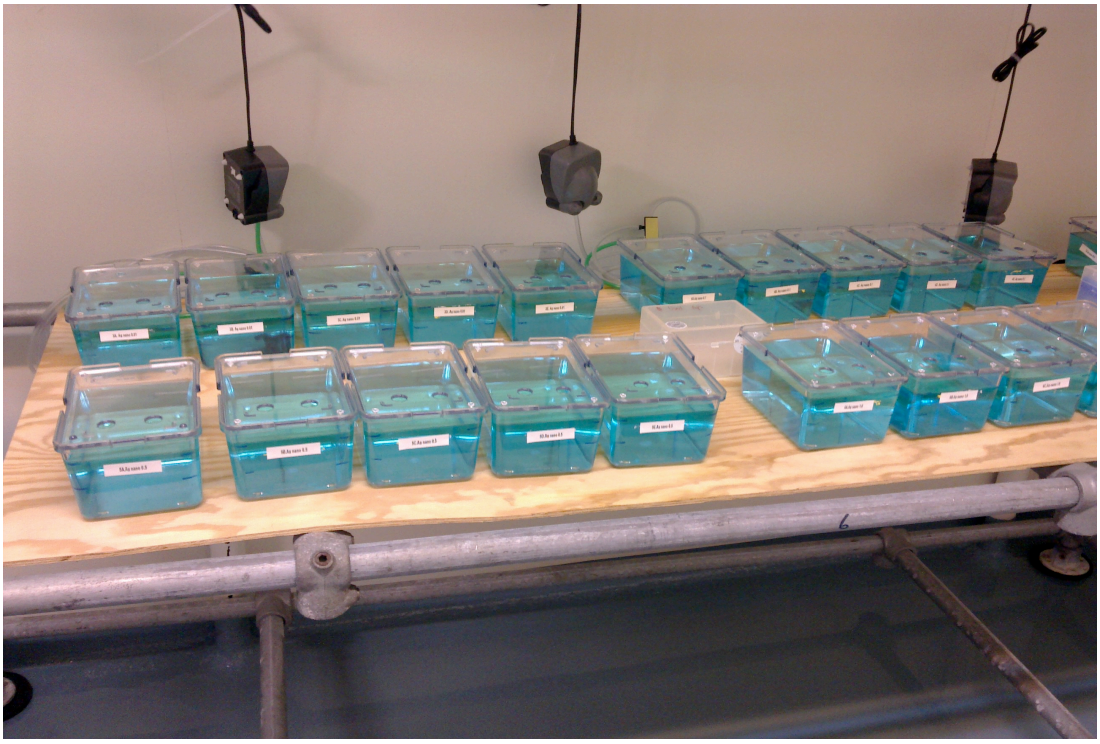

Figure 1. Photography of exposure tanks in the aquaria room in the AZlab.The experimental groups were distributed on two shelves and replicate tanks belonging to the same group were placed together. The air pumps in this photo were not connected to the system. The blue color is from the methylene blue.

2.3.1 Physical and chemical parameters

To ensure optimal conditions the larvae were kept in static tanks with renewal of 50% of the water and respective nominal concentrations on a daily basis. Tanks were changed twice a week. On 6 dpf the experimental tanks were placed in one of the aquaria rooms in the AZlab holding an ambient temperature of 25 ± 1°C and a light: dark regime of 14:10 h. Dead individuals, excess feed and debris were removed on a daily basis with a disposable pipette.

The staff in the zebrafish lab produced conditioned water continuously. Water quality parameters (e.g. pH, NO_2^-, NO_3^-, NH_4^+/NH_3, salinity, degrees of general hardness (GH), degrees of carbonate hardness (KH), temperature and conductivity) were adjusted to be within healthy range prior to use (i.e. conditioned). The temperature in the exposure tanks was measured every day and water quality parameters (e.g. pH, NO_2^-, NO_3^-, NH_4^+/NH_3, GH, KH, O_2 and conductivity) tested on the day of exposure start, 8 dpf and 14 dpf by the Tetra test laborette (GH, KH, NH_4, NO_3, NO_2 and O_2), Hanna instruments (conductivity) and a pH meter.

The recorded values in the experimental tanks were generally within the recommended values of the AZlab (Table 2).

Table 2. Physical parameters in the exposure tanks measured on 6, 8 and 14 dpf. The healthy range is the values recommended in the standard operating procedures of the AZlab.

Parameter	Healthy range*	6 dpf	8 dpf	14 dpf
pH	7-8	7.32	7.22	7.26
NO2- (mg/L)	<0.1	<0.3	<0.3	<0.3
NO3- (mg/L)	<50	0	0	0
NH4+, NH3 (mg/L)	<0.1	0	<0.3	0
dGH	2-8	2	2	2
dKH	3-8	2	2	2
Conductivity (s/cm)	400-600	378	383	413
Temperature (°C)	26-30	26.1	24.0	24.2

* Recommended by the AZlab

2.3.2 Feeding regime

Starting on 6 dpf, the larvae were fed ~ ¼ of a spatula with dry feed (SDS 100, Scanbur AS, Nittedal, Norway) four times a day. To avoid overfeeding, the amount was adjusted on a daily basis by looking for excess feed after 10 min.

From 13 dpf the larvae were fed one droplet of Artemia nauplii (Grade 0, Platinum Label, Argent Laboratories, Redmond, USA) from a disposable pipette twice a day in addition to twice with ~ ¼ of a spatula with dry feed.

2.4 Studied endpoints

2.4.1 Survival

Starting on 6 dpf dead individuals were counted in each replicate tank and survival registered each day until the last day of the study period (21 dpf).

2.4.2 Growth

After the larvae were euthanized at 21 dpf the body length of each larvae were measured with an mm-scaled ruler. The length was measured from the tip of the head to the tip of the

tail as displayed in the Figure 2. A plastic forceps was used to arrange the larvae next to the ruler and the length recorded in centimeters with two decimals.

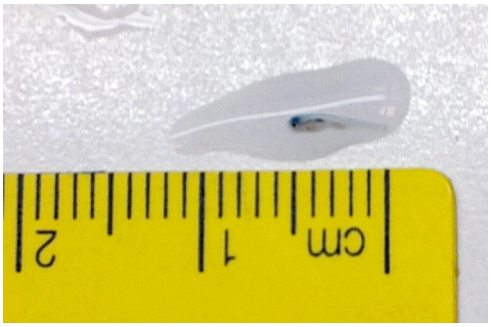

Figure 2. The length of each larva sampled for microarray analysis was measured from head to tail with an mm-scaled ruler as displayed in the photography.

2.5 Microbiological analysis

It was decided to collect water samples (100 mL for each group, consisting of samples of equal amounts from each replicate) for microbiological investigations to be able to investigate whether microbiological contamination could be a potential factor affecting survival.

The samples were plated out on blood agar (BA) and plate count agar (PCA) at room temperature and incubated in 30°C for 24 h before the number of bacterial colonies on each plate were counted manually. Investigations of water samples from the lowest concentration (0.01 mg/L) of silver nanoparticles were not conducted due to problems with the sample preparation for counting. The plating out and microbiological investigations were carried out by staff at the Microbiology and Hygiene laboratory at NVH.

2.6 Sampling and isolation of material for gene expression analyses

On 21 dpf, all fish were euthanized with an overdose of benzocaine (100 mg/mL) in a fish tank placed on ice.

To ensure adequate biological material for the hybridizations six biological replicates were generated from each experimental group by pooling approximately five larvae from each

replicate tank (Figure 3) in 2 mL-tubes containing magnalizer beads (Roche Diagnostics, Oslo, Norway). The number of sampled individuals from each replicate tank was based on the number of larvae that survived the exposure 21 dpf. Samples were snap frozen in liquid nitrogen and stored in – 80°C until required.

2.6.1 Isolation and purification of RNA

All procedures involving nucleic acids were performed with instruments and on benches sterilized with RNeasy away (Qiagen, Oslo, Norway).

Total RNA was isolated with trizol Reagent (Invitrogen, Oslo, Norway), according to the instructions in the manufacturer's manual.

Trizol (1 mL) was added to each tube containing magnalizer beads with frozen tissue and homogenized for 50 sec at a frequency of 25 using a mixer mill (type MM301, Retsch, Dale in Sunnfjord, Norway). The homogenizing was repeated after turning the containers up side down. Samples were allowed to sit for 5 min on ice.

Chloroform (200 µL/mL trizol) was added to the tubes and the solutions were mixed by manually shaking the tubes for 15 sec and incubated for 2 min in room temperature. In order to separate the organic phase from the aqueous phase containing RNA the incubation step was followed by centrifugation at 4000 revolutions per minute (rpm) for 15 min at 2-8°C in a Thermo Scientific Heraeus fresco 21 centrifuge (Fisher Scientifics, Oslo, Norway).

The aqueous phase (500 µL) was added to new micro tubes containing isopropanol of equal amounts as the aqueous phase, incubated for 10 min at room temperature and centrifuged at 4000 rpm for 10 min at 2-8°C. The resulting supernatants were discarded and the precipitated pellets containing RNA were stored in – 75°C.

The next morning the pellets were thawed on ice, vortexed and centrifuged at 4000 rpm in 2-8°C for 5 min. The resulting supernatants were discarded carefully using a pipette and the pellets were left to dry in the tubes. After 5 min RNAse free water (50 µL, Qiagen, Oslo, Norway) was added to each RNA pellet, before the solutions were vortexed. RNA concentrations were measured by a Nanodrop ND-1000 spectrophotometer (Nanodrop Technologies, Delaware, USA) at 260 and 280 nm. Samples (1 µL) of isolated RNA were pipetted on the lower measurement pedestal before the sampling arm was closed and

measurement initiated. Both lower and upper pedestal were cleaned after each measurement using a laboratory wipe.

Absorbance ratios (260 nm/ 280 nm) of 1.8 – 2.0 and yields exceeding 100 ng/µL were considered as acceptable. All values were considered satisfactory (raw data in appendix).

Before proceeding to the purification step, possible genomic contaminations were removed by treating each sample with a mixture of DNase I (2.5 µL DNase I in 10 µL RDD buffer) provided by the RNase-Free DNase set (Qiagen, Oslo, Norway).

To make up a total volume of 100 µL there was added RNase Free water (37.5 µL) to each tube, followed by addition of the mixture of DNase I (12.5 µL). The solutions were incubated for 10 min at room temperature.

Purification of RNA was performed with the RNeasy Mini Kit (Qiagen, Hilden, Germany), according to the manufacturer's protocol. The RNeasy Mini Kit is designed for purification of small amounts of total RNA isolated from animal cells. Messenger RNA (mRNA) is enriched by selective binding of RNA molecules longer than 200 base pairs to a silica membrane in the RNeasy spin columns provided in the kit.

To ensure purification of intact RNA and inactivation of RNase, RLT buffer (350 µL) was added to each sample and the solutions were mixed well by pipetting. Membrane binding conditions were optimized by addition of 96% ethanol (250 µL), mixed well by pipetting and samples (700 µL of each) were transferred to new spin columns, centrifuged at 8000 rpm for 15 sec in the Thermo Scientific Heraeus fresco 21 centrifuge. The centrifugation was repeated after the samples were transferred to new collection tubes.

After columns were transferred to new collection tubes RPE buffer (700 µL) was added and samples centrifuged at 8000 rpm for 15 sec. The flow through from the collection tubes were poured off and spin columns centrifuged at 10 000 rpm for 1 min. Traces of ethanol were removed from the membranes using a pipette and spin columns were transferred to new collection tubes. To elute RNA, RNAse free water (50 µL) was added on top of the membranes and allowed to sit for 2-3 min, followed by centrifugation at 10 000 rpm for 1 min. Spin columns were removed and tubes placed on ice.

Three aliquots of each RNA sample were made by transferring 23 µL sample for microarray analysis, 23 µl for qPCR and 4µL for quantitative and qualitative check for all experimental groups to respective 1.5 mL tubes. Samples were stored in – 75°C until required.

2.6.2 Qualitative assessment of the isolated RNA

Quantity (measured by Nanodrop) and quality of the isolated RNA were measured in order to minimize variations and thereby improving the following labelling and hybridisation process (Forster et al. 2003).

The quality of the purified RNA (1 µL) was examined with the Agilent 2100 Bioanalyzer (Agilent Technologies, California, USA) and the RNA Nano LabChip Kit (Agilent Technologies). The principle of the assay is that fragments of nucleic acids are separated by size as they are driven electrophoretically through interconnected micro channels on a chip.

The 2100 expert software (Agilent) was used to generate electropherograms (Figure 3) and gel-like images. Calculated RNA Integrity Numbers (RINs) and ratios of ribosomal subunits (28s/18s) were used to assess the integrity and detect possible degradation or genomic contamination of the isolated RNA. The software RIN algorithm classify the sample from 1 to 10, with 1 being the most degraded and 10 the most intact. Low ratios of the 28s/18s ribosomal subunits indicate that the samples have been prone to degradation processes.

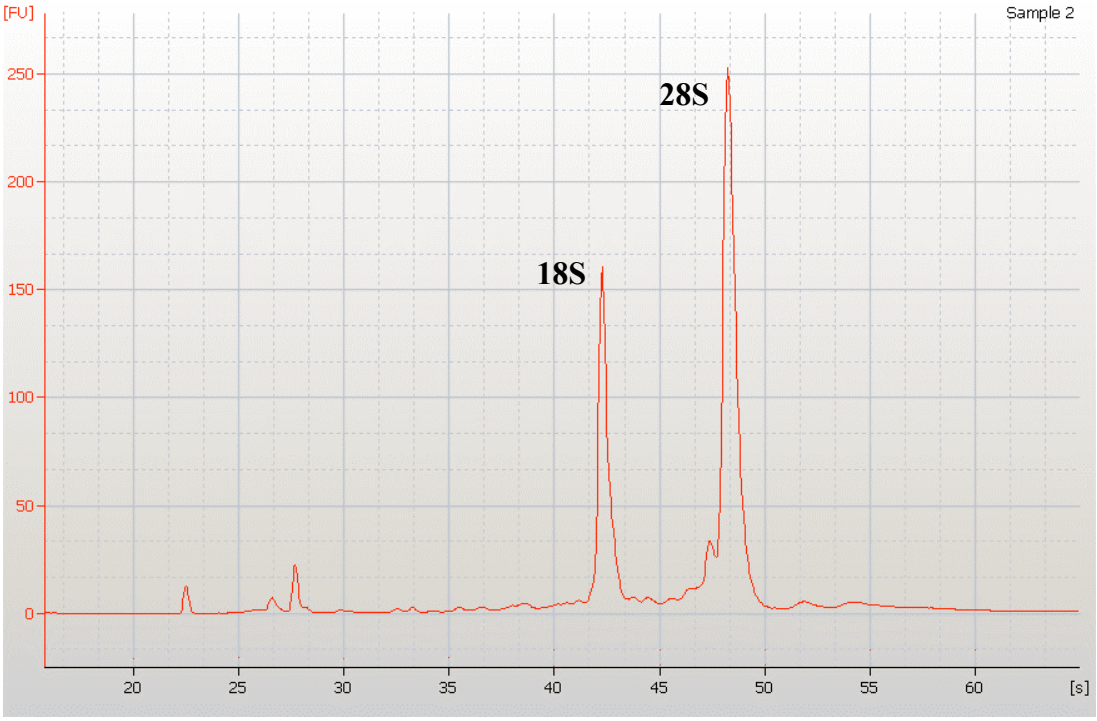

Figure 3. Electropherogram of RNA sample from the control group generated by the Agilent 2100 Bioanalyzer. Integrity time (sec) is displayed on the x-axis and the fluorescence unit (FU) on the y-axis. High quality samples of RNA produce electropherograms with clear 18S and 28S peaks and minimal noise between peaks, as the one displayed here.

The Bioanalyzer results indicated that all samples were of good quality and showed little sign of degradation. Ribosomal ratios ranged from 1.9 – 2.3 and RINs from 7.5 – 10 (mean RIN was 9.5).

2.7 Microarray based gene expression analysis

Agilent's Low Input Quick Amp Labelling kit was used for the amplification and labelling of samples prior to hybridization. Agilent's zebrafish (V3) oligonucleotide microarrays (Matriks AS, Oslo, Norway) were used for the gene expression analysis. One slide consisted of four arrays, with 44 000 probes printed on each array.

2.7.1 Sample preparation and hybridization

Sample labelling, amplification, hybridization and microarray wash were performed according to Agilent's protocol for Two-Color Microarray-Based Gene Analysis (Agilent Technologies, Inc., Santa Clara, CA, USA).

Spike mixes with cyanine-3 (mix A) and cyanine-5 (mix B) provided in the Spike-In kit (Agilent technologies, CA, USA) were diluted to 1:16 in a serial dilution according to the manufacturer's instructions for a starting sample input of 200 ng total RNA and the spike mixes were stored in - 70°C until acquired.

Spike mixes (2 µL) with cyanine 3-CTP (spike mix A) or cyanine 5-CTP (spike mix B) and T7 Promoter Primer Mix (0.8 µL T7 Promoter Primer and 1.0 µL nuclease free water) were prepared and added to each tube according to the dye-swap design (Figure 3). Isolated RNA from the control group was split in two; one half (A-samples) for labelling with Cy3 and the other half with (B-samples) Cy5 to facilitate the dye-swap design. Both samples were made to result in a total of approximately 200 ng input RNA for the labelling reaction and complementary DNA (cDNA) synthesis.

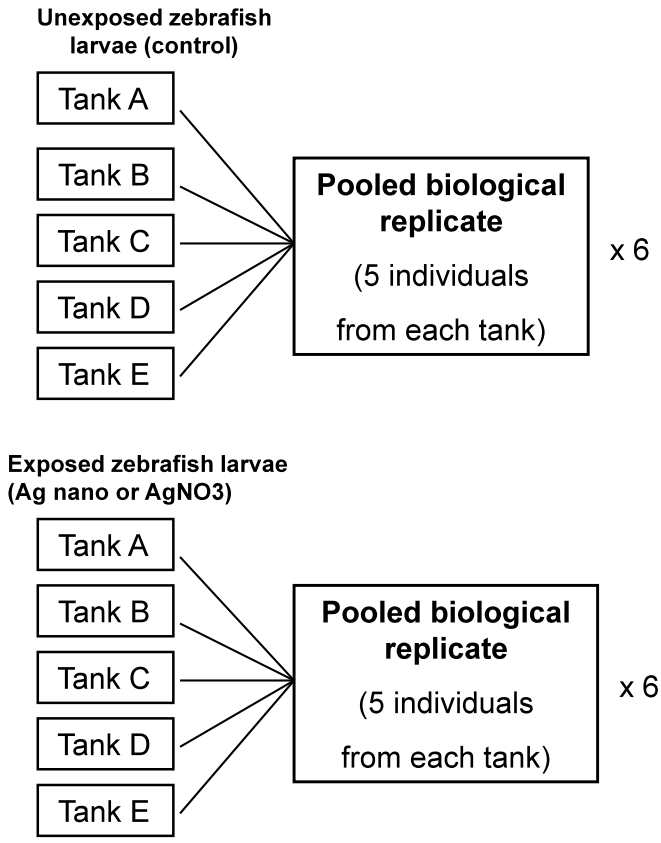

Dye-swap design

Array #	Cy3	Cy5
1	1A	8
2	2A	10
3	3A	12
4	7	4B
5	9	5B
6	11	6B
7	4A	14
8	5A	16
9	6A	18
10	13	1B
11	15	2B
12	17	2B

Figure 4. Microarray design. Approximately 5 larvae were sampled from each replicate tank (Rep. A-E) and pooled in an Eppendorf tube, resulting in one biological replicate. Total RNA from six biological replicates were isolated from each exposure group, purified and labelled with Cy3 (red) or Cy5 (green). Replicates from the control and exposed groups with opposite labels were hybridized on each array (4 arrays on each slide) to achieve a dye-swap experiment. RNA samples from the control group were split in two samples (A and B) with equal concentrations.

To denature the primer and template were each sample incubated at 65°C for 10 min before they were placed on ice for 5 min. A cDNA master mix (4.7 µL) containing 5X First Strand Buffer (54 µL), 0.1 M DTT (27 µL), 10 mM dNTP mix (13.5 µL) and AffinityScript Rnase Block Mix (32.4 µL) was added to each tube and the solutions were mixed by pipetting before incubated in a water bath holding 40°C for 2 h, followed by incubation in another water bath of 70°C for 15 min. After incubation the samples were placed on ice for 5 min and spinned down in a microcentrifuge (Galaxy mini, VWR International, Oslo Norway). The cDNA samples were stored in - 80°C over night.

On the next day complementary RNA (cRNA) was synthesized by adding Transcription master mix (6 µL) to each tube. The Transcription master mix was made of nuclease free water (0.75 µL), 5X First Transcription Buffer (3.2 µL), 0.1 M DTT (0.6 µL), NTP mix (1 µL), T7 RNA Polymerase Blend (0.21 µL) and cyanine 3-CTP or cyanine 5-CTP (0.24 µL) provided in the kit. The solutions were mixed by pipetting and incubated for 2 h at 40°C in a circulating water bath.

The Qiagen RNeasy mini kit was used to purify the amplified and labelled cRNA samples, according to the kit's manual. To make up a total volume of 100 µL, nuclease free water (84 µL) were added to the cRNA samples before proceeding with the purification step. RLT Buffer (350 µL) and 96 % ethanol (250 µL) was added to the tubes and mixed well by pipetting. The cRNA samples (700 µL) were transferred to RNeasy mini columns and centrifuged at 13 000 rpm for 30 sec at 4°C. The RNeasy columns were transferred to new collection tubes (2 mL), RPE Buffer (500 µL) was added and the centrifugation step repeated before the flow-through in the collection tubes were discarded. Fresh RPE buffer (500 µL) was added and the samples were centrifuged at 13 000 rpm for 1 min at 4°C before the flow-through and the collection tubes were discarded. Any traces of RPE buffer were removed by a pipette and the cRNA samples eluted by addition of RNase free water (30 µL) on the RNeasy filter membrane and allowed to sit for 1 min. This was followed by centrifugation at 13 000 rpm for 30 sec at 4°C. The flow-through containing the cRNA was kept on ice and columns were discarded.

The Nanodrop spectrophotometer was used to quantify the labelled and amplified cRNA (1 µL). The recorded dye concentration (pmol/µL) of Cy3 or Cy5, RNA absorbance ratio (260 nm/280 nm) and cRNA concentration were used to calculate and examine the yield and specific activity of each reaction as described in the appendix. Recommended yield was

0.825 µg and specific activity recommended to 6 pmol Cy3 or Cy5 per µg cRNA. The yield and specific activity ranged from 223 – 521 µg and 27.4 – 37.4 pmol dye per µg cRNA respectively and satisfied the recommended values. The labelled and amplified samples were stored in -70°C until acquired for hybridization.

To ensure a sample input of 825 ng cRNA for the hybridization the yield and specific activity quantified by Nanodrop were used to calculate the volume of prepared cRNA to be added to each microarray (calculations in appendix). Sterile 1.5 mL microcentrifuge tubes were prepared for each hybridization and 10X Blocking Agent (11 µL), 25 X Fragmentation Buffer (2.2 µL), nuclease free water (to make a total volume of 52.8 µL) were added to each tube together with the calculated volume of Cy3-labelled cRNA and Cy5-labelled cRNA. Samples were mixed on a Labinco L46 vortexer, incubated at 60°C for 30 min and cooled on ice for 1 min in order to fragment the RNA.

The 2x Gee Hybridization Buffer HI-RPM (55 µL) provided in the kit was added to each tube to stop the fragmentation reaction and the solutions were mixed by carefully pipetting the solutions up and down. The samples were centrifuged at 13 000 rpm for 1 min at room temperature and placed on ice.

Prepared samples (100 µL) were loaded on respective gasket slides using a micropipette before they were covered with the slides containing the microarrays, with the active side towards the samples. The slides were placed in a SureHyb hybridization chamber (Agilent technologies) and hybridized in an Agilent hybridization oven at 65°C for 17 h. Rotation was set to 10 rpm.

To reduce possible array wash artefacts there were added 10% Triton X-102 (2 mL) provided in the kit to the Gene Expression Wash Buffer 1 and 2. The Gene Expression Wash Buffer (GE Wash Buffer) 2 was heated over night in a water bath holding 37°C. Wash buffers and solutions for washing the microarray slides were prepared in separate 50 mL Falcon tubes. After the slides were hybridized in the hybridization oven for 17 h they were placed in a Falcon tube containing the GE Wash Buffer 1 at room temperature and the gasket slide were removed with a plastic tweezer. The liquid covered the slides. The slides were transferred to a second tube with GE Wash Buffer 1 and washed for 1 min at room temperature, followed by a wash for 1 min in a tube containing the GE Wash Buffer 2 (37°C) and finally for 30 sec at room temperature in a tube with Stabilization and Drying

solution provided in the kit. The wash procedures were carried out in 50 mL Falcon tubes covered in foil on a roller mixer (Stuart scientific SRT1, Sigma Aldrich, UK).

2.7.2 Microarray scan

The hybridized slides were scanned using the GenePix 4000B scanner (Molecular Devices, CA, USA) and the fluorescence intensity of each dye at each spot on the arrays were processed in the GenePixPro 6.0 software in order to quantify the relative abundance of the corresponding cDNA probe in the exposed vs. control samples (Dudoit et al. 2002). The scanner acquired data from two wavelengths simultaneously by dual photomultipliers (PMTs), and the PMT gain values were automatically selected by the scanner. The intensity of each spot was adjusted manually to a level close to the saturation level in to minimize background signals, maximize spot intensity and avoid saturated (white) spots (Forster et al. 2003) and the ratios of red (Cy3) and green (Cy5) dye were calculated by the GenePixPro software. A GenePix Array List (GAL) was uploaded to the software and fitted to each of the images to name and identify each spot on the arrays before further processing of the microarray data.

2.8 Normalization and analysis of microarray data

The raw data were log transformed ($\log_2$) in order to get a more symmetrically representation of the intensity ratios. Negative values of red (R) or green (G) intensities were removed from the data set (Dudoit et al. 2002; White & Salamonsen 2005) before the fluorescence intensities were normalized within arrays (print-tip group locally weighted scatterplot smoothing) and between arrays (scale) in the linear models for microarrays Graphical User Interface (limmaGUI) package produced for Bioconductor's R environment to eliminate systemic variations in the dataset (Smyth & Speed 2003; Wettenhall & Smyth 2004). A RNA Target file, GAL file and Spot Type file were uploaded to limmaGUI as tab-delimited text files.

The limmaGUI package fits a linear model to the data, tests the hypothesis that the expression values of the genes in the exposed groups is equal relative to the expressions in the unexposed and adjust the p-values for multiple testing (Smyth 2004; Wettenhall & Smyth 2004).

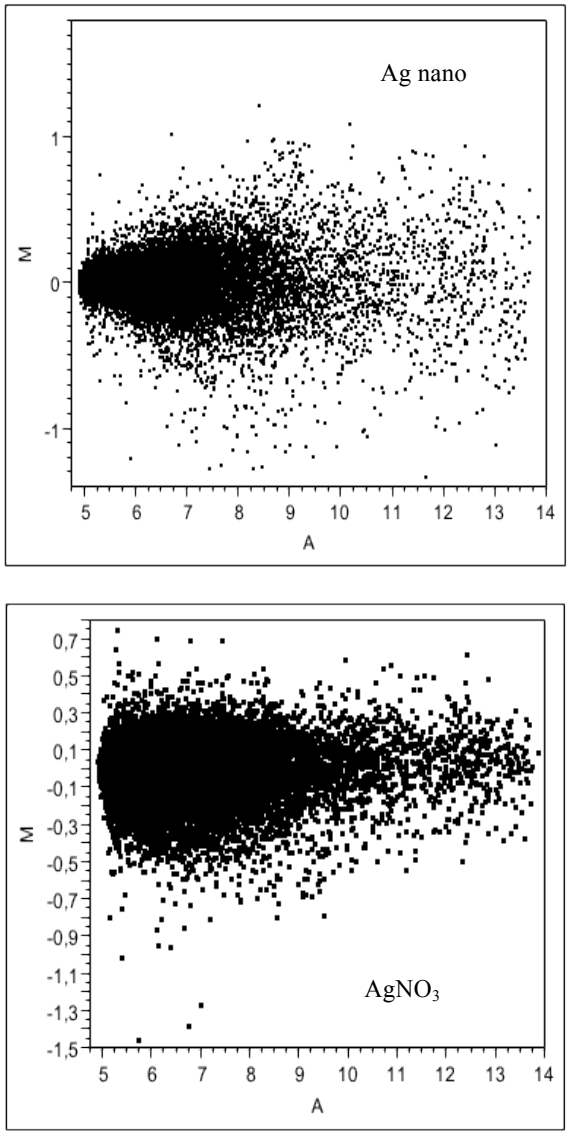

Figure 6. MA-scatter plots of log-transformed (log_2) intensity ratios from the microarray scan for the silver nano (0.01 mg/L) group (top) and silver nitrate (0.01mg/L) group (bottom). Y-axis represents the intensity log ratio (M) and the x-axis represents the mean log intensity (A). Genes with low fold change ratios are centred around M=0.

The normalized intensity log-ratios $M=\log_2 R/G$ (y-axis) and mean log intensity $A=\log_2 \sqrt{R/G}$ (x-axis) for each probe were plotted in a scatterplot (MA-plot) by a bivariate fit of M by A for the two exposed groups and used to set threshold values for excluding genes with low intensity ratios (low expression) and genes with low fold change values (log ratios).

Genes with M values between +0.3 and -0.3 and mean log intensity <6 (low intensity) were excluded from the gene lists, before genes assigned adjusted p-values ≤0.05 were selected for further analyses in the Ingenuity Pathway Analysis (IPA) software.

2.9 Analysis of changes in gene expression

The lists of the differently expressed genes, corresponding log ratios and adjusted p-values were uploaded to the IPA software to examine responses in the transcriptome after exposure to silver nanoparticles and silver nitrate, and to identify the unique and common genes across the two datasets.

Each identifier was mapped to corresponding human, rat or mouse homolog in the Ingenuity Knowledge Base and the Core Analysis was used to identify molecular functions, canonical pathways, biological functions and diseases most significantly associated with the two exposures. Functions and pathways associated with molecules identified to be unique for the two exposures were further explored.

2.10 Validation of microarray results by qPCR

A total of 10 target genes (Table 3) were randomly selected from the microarray generated gene lists for validation of the fold change measured by the microarrays.

The Superscript III Platinum Two-step qRT-PCR kit with SYBR Green (Invitrogen, Life technologies, Norway) was applied for real-time quantification of fold change of 10 target genes in aliquots of the same total RNA samples that were used for the microarrays. The kit enables a simple, sensitive and reproducible quantification of RNA by the 7900 HT Fast Real-Time PCR System (Applied Biosystems, Life technologies).

The Universal ProbeLibrary Assay Design Center software (Roche Applied Science version 2.45) was applied to design suitable target specific qPCR primer pairs for the selected genes (Table 3). The designed primer pairs were ranked by the software using optimized default settings and the top ranked intron-spanning primers closest to the 3'end with an amplicon size less than 120 base pairs were selected for the qPCR analysis.

Table 3. Selected genes and designed primer pairs for validation of the microarray results by qPCR.

Gene name	Gene	Forward primer (5'-3')	Reverse primer (5'-3')
ATP-binding cassette, sub-family A (ABC1), member 1	*ABCA1*	cttaccctggccaagtgc	aaccaggatgctgaccagac
B-cell receptor-associated protein 31	*BCAP31*	gatgccgccaagaaatacat	cacttcaataccggcttgc
Biorientation of chromosomesin cell division 1	*BOD1*	aaattcagcccctgatgttg	ggcaaaaatccttggacctc
Phosphogluconate dehydrogenase	*PGD*	tgacgggtacagacacgaga	gtgcgcaccaaagtagtctct
Zinc fingers and homeoboxes 2	*ZHX2*	ccgagaccttgaagtgctgt	catagcagccttttttccttcttt
Aminolevulinate, delta-, synthase 1	*ALAS1*	ggtcatgcacaagatggaca	atgtacccgcccacacag
Antizyme inhibitor 1	*AZIN1*	tgaacgatggtgtttatggatct	tcatctagggtgagcgacatc
Hematological and neurological expressed 1	*HN1*	gaacccgaggaccctcat	gcagatggttctccacacaac
Heat shock 70kDa protein 4	*HSPA4*	aagacactgaggtctggctgta	gggttggccaaggttctt
Insulin induced gene 1	*INSIG1*	atcaatcacgccagtgctaa	accacagacccagagacagg

The qPCR assay was optimized in regard of annealing temperature (e.g. 60°C) and the amplicons were tested by a 2% agarose gel electrophoresis. The gel was made by mixing 2% LE agarose (SeaKem, MedProbe, Oslo) with TAE buffer (100 mL) and stained by adding 2 droplets of ethidium bromide (0.6 mg/L stock solution). Examination of the photography showed single bonds of expected size.

Each primer pair was tested with four different concentrations of complementary DNA (cDNA); 10 ng/µL, 5 ng/µL, 2.5 ng/µL and 1.25 ng/µL to find the optimal concentration for further analyses. Both 2.5 ng/µL and 1.25 ng/µL gave satisfactory treshold cycle (C_T) values between 17-30 for all primer pairs and 1.25 ng/µL was selected for further work.

The amplification efficiency for each primer pair was tested with a 10 fold dilution series (e.g. 30 ng/µL, 3 ng/µL, 0.3 ng/µL, 0.03 ng/µL and 0.003 ng/µL) of one control sample and two exposed samples (Ag nano and $AgNO_3$). A standard curve for each primer pair was generated and the slopes were used to calculate the amplification efficiencies (E). The calculated mean efficiency ranged from 1.91 to 2.19, which means that the templates were approximately doubled for each amplification cycle and with >91% efficiency.

Isolated total RNA (with known concentrations) from the experimental groups were used for cDNA synthesis. RNA samples (4µL) were reverse transcribed to cDNA in respective wells on a 96 well PCR plate on ice using the master mix (16 µL) provided by the Superscript III Platinum Two-step qRT-PCR kit (Invitrogen).

The master mix was made by mixing 2X Reverse Transcription (RT) Reaction Mix (10 µL), RT Enzyme Mix (2 µL) and RNase Free water (4 µL) in Eppendorf tubes on ice for each reaction, with 11 reactions in total.

The plate was centrifuged for 1 sec at 2000 rpm in a megafuge (Heraeus sepatech). First-strand cDNA was synthesized in a Peltier Thermal Cycler-225 (MJResearch, Waltham, MA, USA); 10 min at 25°C, 42°C for 50 min, and 85°C for 5 min before the plate was chilled on ice. To exclude traces of RNA, the plate was treated with RNase H (1 µL) and incubated at 37°C for 20 min. The cDNA was diluted in RNase free water to 1.25 ng/µL and stored at -20°C until required.

2.10.1 Real-Time Quantitative Polymerase Chain Reaction

The qPCRs for the 10 target genes were performed using SYBR Green. A master mix was made up for each primer pair with components provided in the SYBR Green RT-PCR Reagents kit (Applied Biosystems). The master mix contained SYBR Greener qPCR supermix (10 µL), 10 µM forward primer (0.5 µL), 10 µM reverse primer (0.5 µL) and RNase Free water (4 µL) that were mixed for each reaction in Eppendorf tubes on ice. Master mixes were added to each well (15 µL in each well) together with respective samples of previously synthesized cDNA (5 µL) on 96 well PCR plates on ice. Negative controls without reverse transcriptase (neg-rt) and master mix without template (neg-temp) were included on the plates to control the samples for genomic contamination (neg-rt) and generation of primer dimers (neg-temp). All samples were run in triplets. The plates were sealed with sterile plastic films, centrifuged for 1 sec at 2000 rpm and the assays were carried out in a Real-Time PCR machine (7900 HT Fast real-Time PCR System, AB Applied Biosystem) operating by the SDS 2.3 software (Applied Biosystems): 50°C for 2 min (UDG incubation), 95°C for 10 min (enzyme activation), 95°C for 15 sec (denaturation) and 60°C for 1 min (annealing and elongation).

Dissociation curves were included in the end of each run to identify possible contaminations or formation of primer-dimers. A single peak at the melting temperature of the amplicons was observed for all plates as the one presented for the control samples and *β-actin* (Figure 7), and indicate the absence of contaminations and primer-dimers.

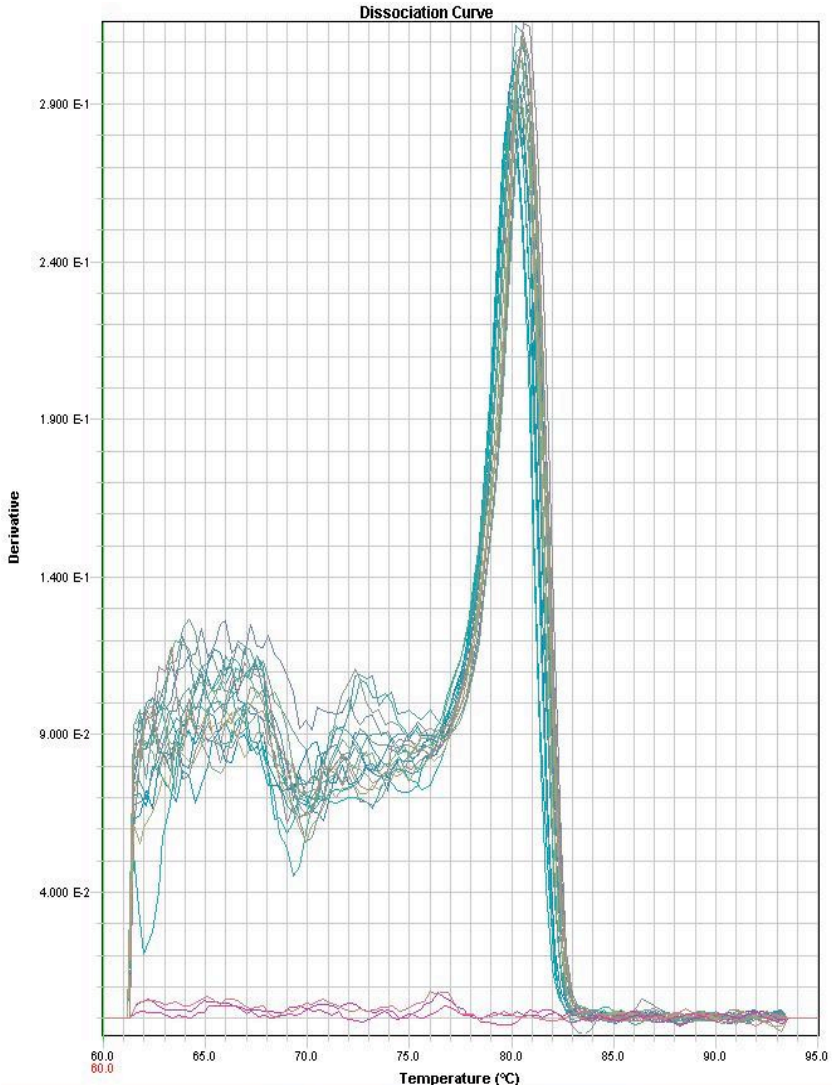

Figure 7. Dissociation curve generated from the qPCR of the control samples and the reference gene (*β-actin*). The single peak at the amplicon's melting temperature indicate absence of contamination and primer-dimers.

Reference genes are used for normalization prior to relative quantification of gene expression data and should not be affected by the treatment. The C_T values generated for six in-house zebrafish housekeeping genes (β-*ACTIN*, *EF1*α, *GAPDH*, *RNAP*, *RPL13*α and *SDHA*) were analyzed in the GeNorm software (PrimerDesign Ltd, Southampton, UK) to identify the optimal normalizing gene for qPCR data using SYBR Green. The tested genes have been evaluated as suitable reference genes for zebrafish material and the stability of more than one reference gene were tested as recommended prior to a new qPCR assay (Tang et al. 2008).

The C_T values were transformed into relative expression values by the ΔC_T method described in the GeNorm Housekeeping Gene Selecting Kit Handbook (07/07) before the data were uploaded to the GeNorm software. The genes were ranked from left to right on a graph (Figure 8), with the highest expression stability to the right.

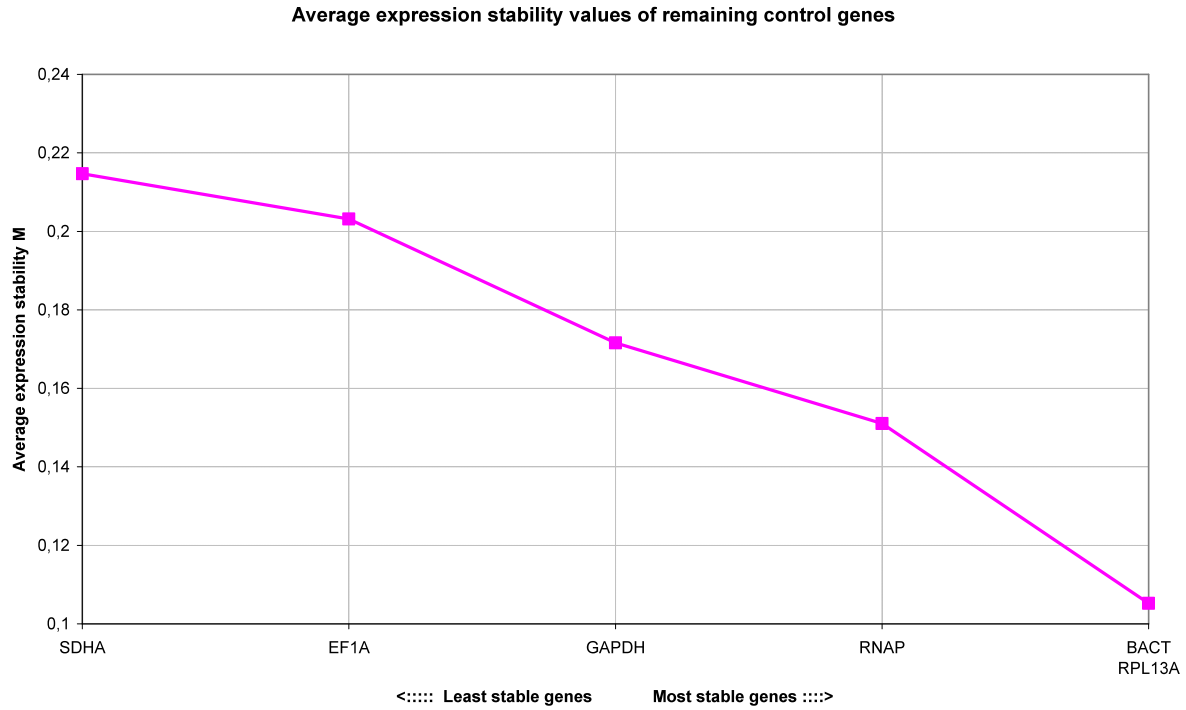

Figure 8. Graph generated by the GeNorm software, which ranked the reference genes under investigation based on their average expression stability. The y-axis displays the average expression stability and the genes with increasing expression stability is ranked to the right on the x-axis.

Of the most stable genes, it was β-*ACTIN* that was assessed to be among the most stable genes with average expression stability <0.22 and the lowest gene expression stability value and were selected for normalization of the gene expression data generated by the qPCR assays.

The raw data generated in the SDS 2.3 software were uploaded to RQ manager 1.2 and the treshold was set manually for all genes. The β-*ACTIN*-normalized C_T values were analyzed in Microsoft Excel 2003 by the Livak method (Livak & Schmittgen 2001) in order to determine the mean fold change of the target genes in the exposed samples relative to the fold change in the control group. Amplification efficiency near 100% of both target and reference genes are assumed in the Livak method and was verified by the previously performed serial dilutions.

2.11 Statistical analyses

The statistical analyses were performed in Microsoft Exel 2003 and JMP 8.0 software (SAS Insitute Inc., Cary, NC, USA), and p-values ≤ 0.05 were considered as significant.

Kaplan-Meier survival curves (proportion of survival at each time point) were estimated for all groups and the differences in survival between unexposed and exposed groups were investigated by the log-rank test (Kleinbaum & Klein 2005). The Cox's (semi-parametric) proportional hazard model and likelihood ratio statistics (Kleinbaum & Klein 2005) were used to investigate the replicate tank effect. The nested analysis of the interacting effects of replicate tanks within exposures showed that this interaction was insignificant ($p=0.86$). The results include estimated risk ratios for all groups, which were estimated by comparing the survival (time to death) in the unexposed group versus survival in exposed groups. Risk ratios larger than 1 implies an increased risk in the exposed groups compared to the control (Cantor 2003; Kleinbaum & Klein 2005).

Levene's test was used to assess the homogeneity of variance in the length data and indicated an unequal variance. Mean length within replicate tank was used as observational unit it the statistical analyses. Differences in the mean length recorded in the exposed and unexposed groups were analyzed by Welch ANOVA (which allows unequal variance across group), before all groups were compared to control by non-parametric Kruskal-Wallis test.

Student's t-test was used to compare the differences in the mean $\log_2$ transformed fold change ratios of the 10 target genes analyzed by qPCR in the exposed groups versus the unexposed control (n=6).

3. Results

3.1 Characterization of size and size distribution

Large particles with mean hydrodynamic diameters of 484 nm were found in the sample of conditioned water (appendix A).

Table 4. Intensity-weighted mean hydrodynamic diameters (Z.avg), polydispersity indexes (PDI) and photon count rate (kilo-counts per second).

Sample	Z.avg (d.nm)	PDI	Count rate (kcps)
Control 0 mg/L	1713	0,57	338
Ag nano 0.01 mg/L	1345	0,37	142
Ag nano 0.1 mg/L	227	0,37	157
Ag nano 0.5 mg/L	179	0,33	114
Ag nano 1.0 mg/L	165	0,37	315

PDI values >0.1 indicate that there was a wide distribution of size in all samples. All samples contained particles of mean hydrodynamic diameters >100 nm.

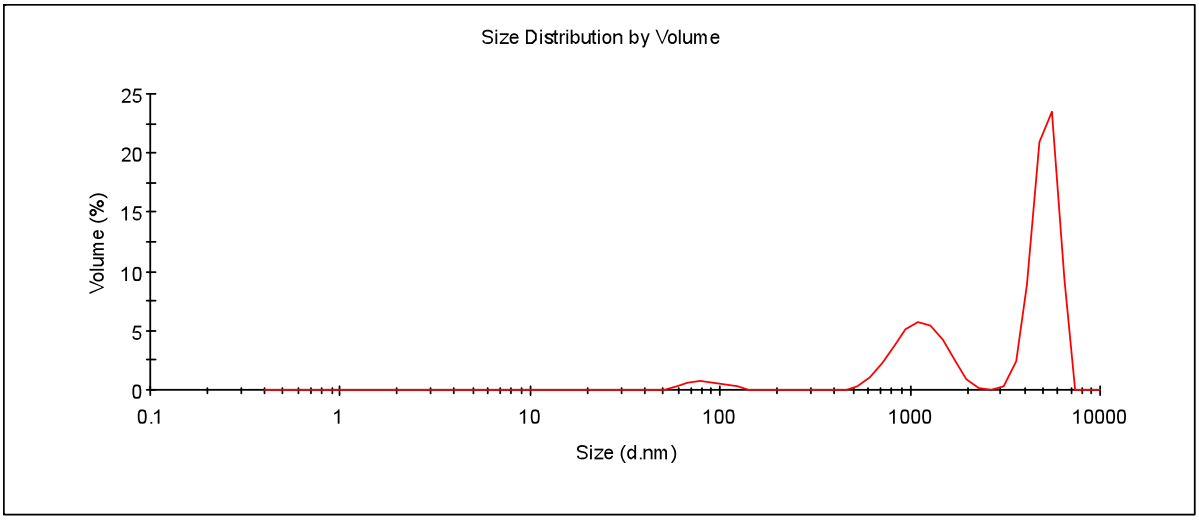

Figure 9. Volume distributions of relative light scattered by populations of particles in various size classes in the sample collected from the control group exposed to 0.0 mg/L silver nanoparticles. The y-axis shows the relative intensity of scattered light and particle size is presented on a logarithmic x-axis.

Mean size of the particles contributing to the three peaks displayed in Figure 9 were reported to be 87 nm, 1159 nm and 5163 nm, respectively.

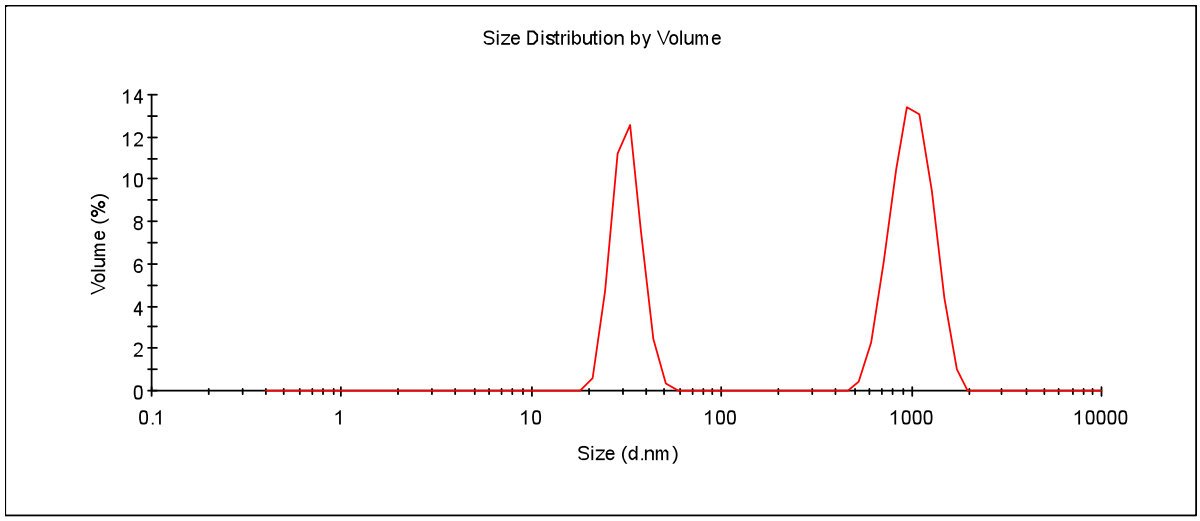

Figure 10. Volume distributions of relative light scattered by two populations of particles in various size classes in the sample collected from the group exposed to 0.01 mg/L silver nanoparticles. The y-axis shows the relative intensity of scattered light and particle size is presented on a logarithmic x-axis.

Mean size of the particles contributing to the two peaks displayed in Figure 10 were reported to be 32 nm and 1026 nm for the left and right peaks, respectively.

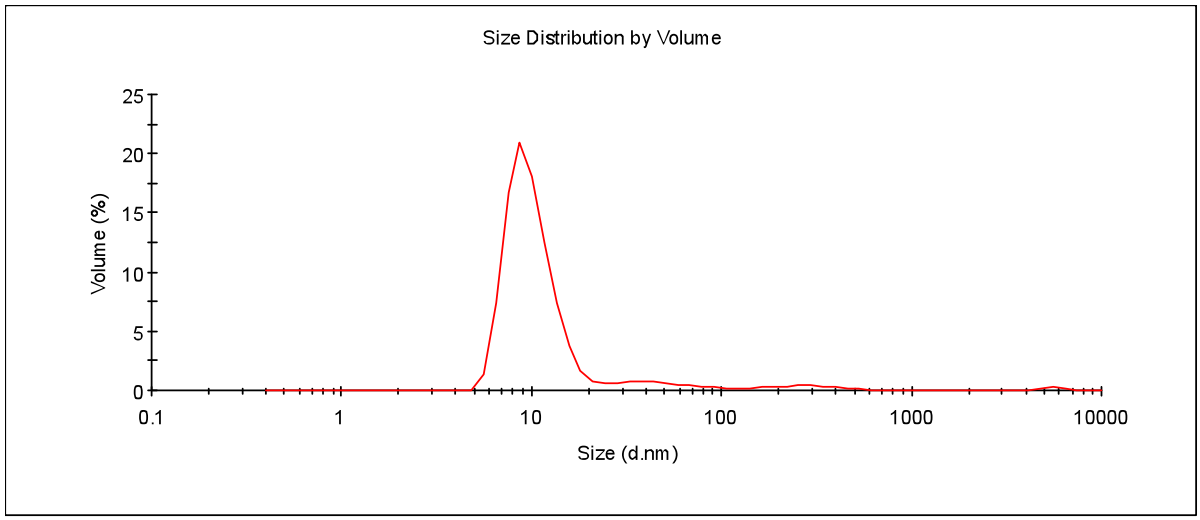

Figure 11. Volume distributions of relative light scattered by particles of various size in the sample collected from the group exposed to 0.1 mg/L silver nanoparticles. The y-axis shows the relative intensity of scattered light and particle size is presented on a logarithmic x-axis

Mean size of the particles contributing to the peak displayed in Figure 11 was reported to be 10 nm.

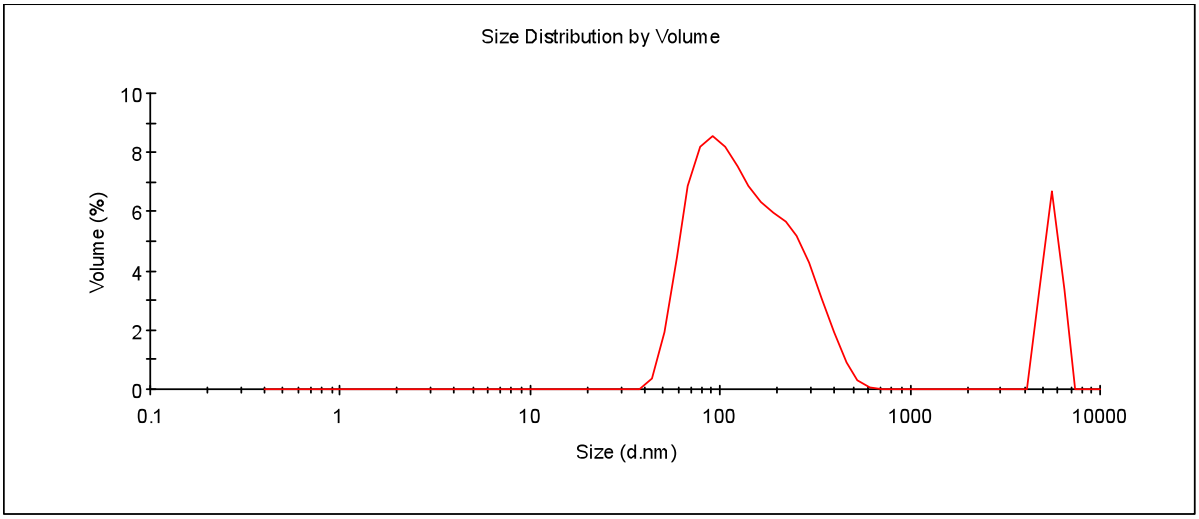

Figure 12. Volume distributions of relative light scattered by two populations of particles in various size classes in the sample collected from the group exposed to 0.5 mg/L silver nanoparticles. The y-axis shows the relative intensity of scattered light and particle size is presented on a logarithmic x-axis

Mean size of the particles contributing to the two peaks displayed in Figure 12 were reported to be 155 nm and 5590 nm for the left and right peaks, respectively.

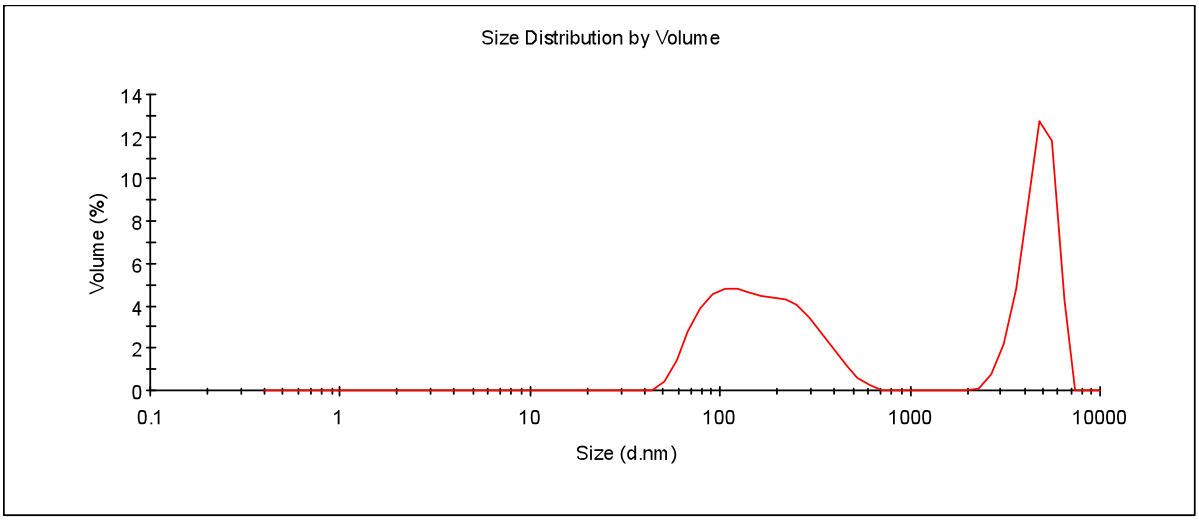

Figure 13. Volume distributions of relative light scattered by two populations of particles in various size classes in the sample collected from the group exposed to 1.0 mg/L silver nanoparticles. The y-axis is the relative intensity of scattered light and particle size is presented on a logarithmic x-axis.

Mean size of the particles contributing to the two peaks displayed in Figure 13 were reported to be 184 nm and 4777 nm for the left and right peaks respectively.

Examples of the studied TEM images are presented in Figures 14 and 15.

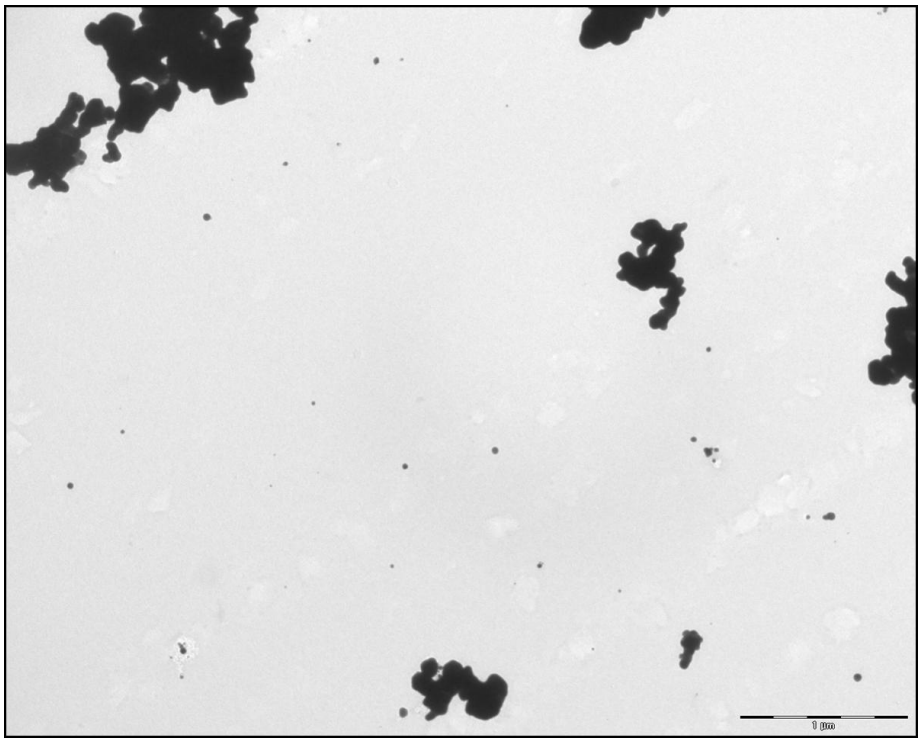

Figure 14. Representative TEM image (14 kx magnification) of nanoparticles in the stock solution (1000 mg/L by mass of nanoparticles). Silver particles can be seen in black against the grey background. The scale bar is 1 μm, with black and white fields equal to 200 nm.

The 14 kx magnification (Figure 14) of the dehydrated sample of the stock solution shows the presence of smaller particles in <200 nm and agglomerates.

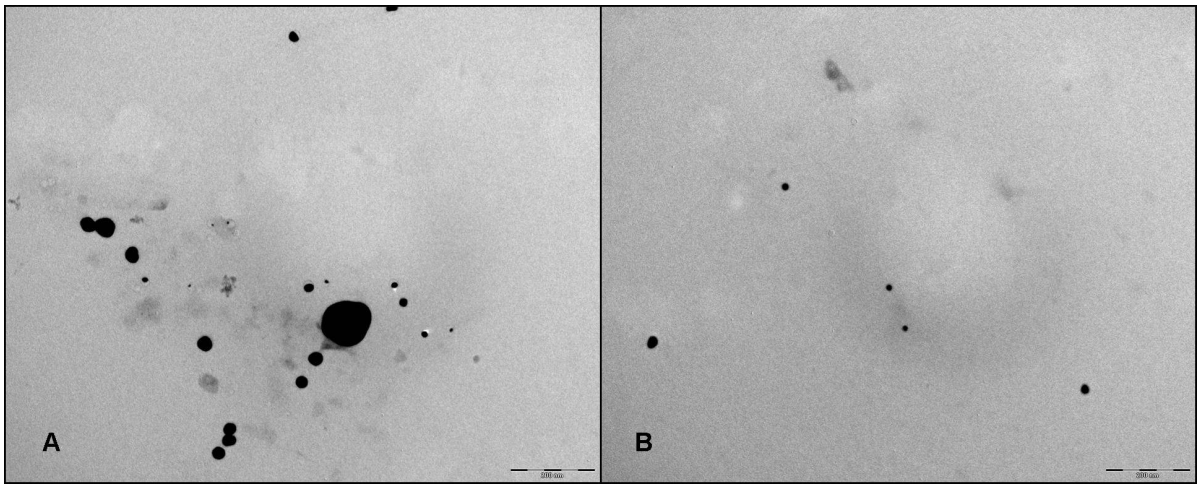

Figure 15. Magnified (56 kx) TEM images of nanoparticles in the stock solution (1000 mg/L by mass of nanoparticles). Silver particles can be seen in black against the grey background. Scale bars are 200 nm, where each black or white field is 40 nm.

TEM assessments of the stock solution at higher magnification identified agglomerates and smaller nanoparticles <40 nm.

3.2 Survival

Kaplan-Meier plots (Figure 16) generated from the censored data depicts the differences in survival proportions in all groups at each time point during the study period. The log-rank test indicated that there was a significant difference between the survival curves of the group exposed to a nominal concentration of 1.0 mg/L by mass of silver nanoparticles compared to the control (log-rank p-value <0.01).

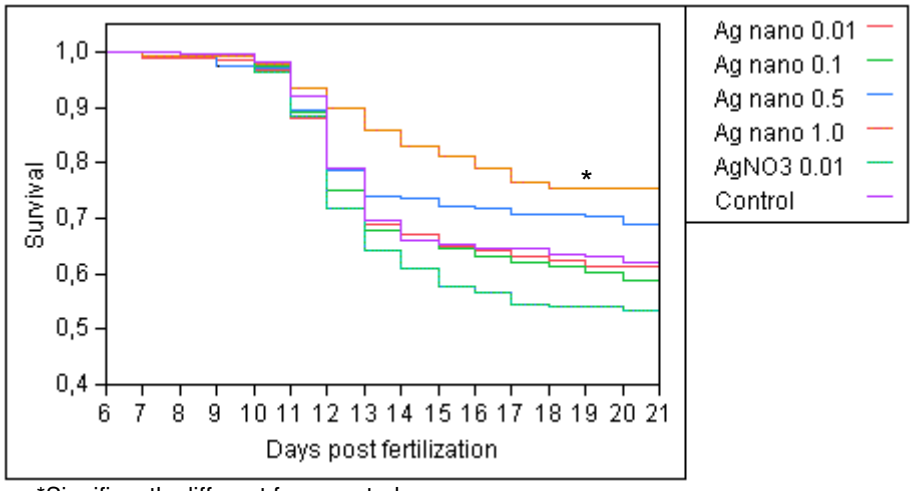

*Significantly different from control

Figure 16. Plot of Kaplan-Meier estimates of the survival proportions at any observed time point from 6 dpf until 21 dpf in the respective groups. Time is represented by jump points and proportion of survival is represented by horizontal lines. The red curve represents the survival function of the control group (0 mg/L). It should be noted that the axes intercepts at y=0.4.

Estimated survival curves descended rapidly around 11-12 dpf and flattened out around 16 dpf in all groups. Percentage survival registred in the control group on 21 dpf varied around 60 ±2% of the survival on 6 dpf.

The likelihood ratio statistics identified exposure to be a significant explanatory variable for the overall differences in survival times (p-value <0.0001) and the significance of the replicate tank variable was found to be insignificant within all groups.

Table 5. Estimated risk ratios, parameter estimates (β), standard error (SE) and significance of the exposure for the differences in the survival time compared to the survival in the control.

Experimental group	n	β	SE	Risk ratio	p-value
$AgNO_3$ 0.01 mg/L	520	0.10	0.07	0.83	0.16
Ag nano 0.01 mg/L	520	-0.01	0.07	0.01	0.93
Ag nano 0.1 mg/L	520	0.05	0.07	0.91	0.48
Ag nano 0.5 mg/L	520	-0.12	0.07	1.26	0.11
Ag nano 1.0 mg/L	520	-0.28	0.08	1.76	<0.01*

* Significantly different from the survival in the control

There were estimated risk ratios >1 for the groups exposed to 0.5 mg/L and 1.0 mg/L silver nanoparticles. Exposure to 1.0 mg/L AgNPs was revealed to have a significant effect on the survival of zebrafish larvae exposed from 6 dpf – 21 dpf.

3.3 Growth

In order to detect any significant effects on growth (e.g. body length) after exposure to four concentrations of silver nanoparticles or silver nitrate (0.01 mg/L) the mean length in each replicate tank was measured on 21 dpf (Table 6).

Table 6. Recorded mean body length (cm) on 21 dpf after exposure to silver nanoparticles (Ag nano) or silver nitrate ($AgNO_3$) from 6 dpf – 21 dpf. N=number of larvae exposed from the beginning of the study period. The Kruskal-Wallis' ANOVA p-values indicate if the mean length of the exposed larvae was significantly different from the control.

Experimental group	n	Mean	SEM	p-value
Control	5	0.486	0.005	
$AgNO_3$ 0.01 mg/L	5	0.474	0.003	0.12
Ag nano 0.01 mg/L	5	0.492	0.004	0.35
Ag nano 0.1 mg/L	5	0.494	0.003	0.21
Ag nano 0.5 mg/L	5	0.489	0.006	0.68
Ag nano 1.0 mg/L	5	0.483	0.003	0.60

No significant differences were found in the mean length between replicate tanks in any of the groups (p-values> 0.05).

3.4 Microbiological analysis

Total number of bacterial colonies in samples from each group incubated on blood agar and plate count agar.

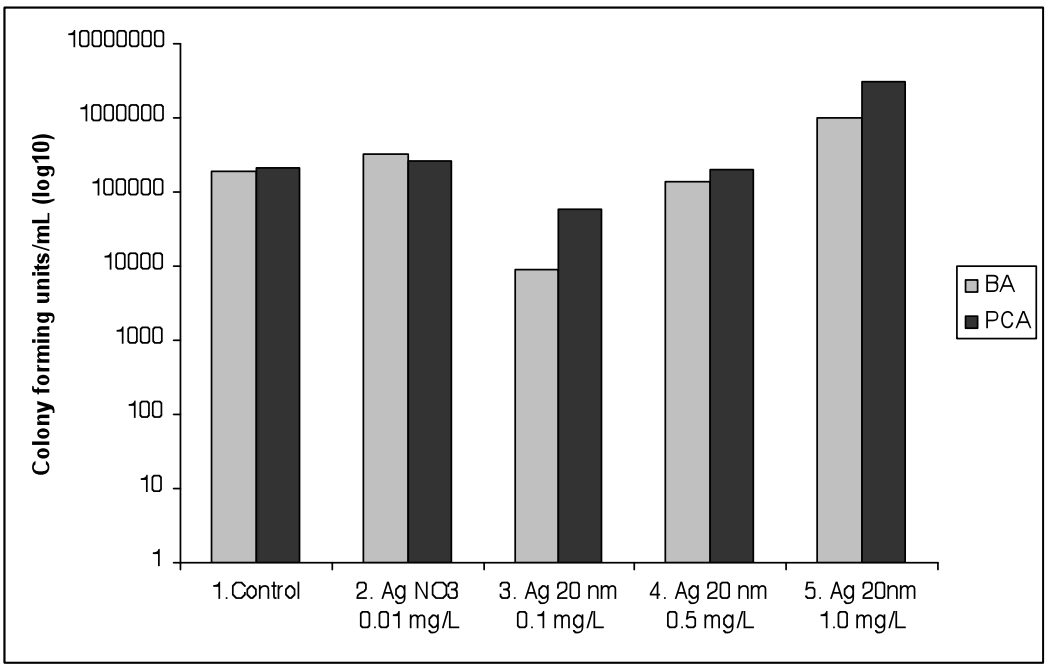

Figure 17. Number of colony forming units per mL (y-axis) counted in water samples (x-axis) incubated at 30°C for 24 h on blood agar (BA) and plate count agar (PCA). The y-axis is in the logarithmic scale to base 10.

The highest number of colonies per mL was counted in the water sample from the group treated with 1.0 mg/L silver nanoparticles, with 1.02 $x10^6$ and 3.04 $x10^6$ bacterial forming units per mL after incubation for 24 h on BA and PCA respectively.

3.5 Changes in gene expression

A total of 65 genes (appendix D) were found to be significantly affected by the exposure to silver nanoparticles (0.01 mg/L) relative to control (adjusted p-value <0.05), and a total of 7 genes (appendix E) by the same concentration of silver nitrate.

Analyzes of the gene expression profiles revealed that 31 of the identified genes were unique for the group exposed to nanoparticles (Table 7), whilst silver nitrate did only significantly affect the transcription of 2 unique genes (Table 8). Two genes were found to be significantly induced in both exposures, i.e. *glycoprotein 2* (GP2) and *phosphodiesterase 6H* (PDE6H).

Table 7. Unique genes affected in larvae exposed to silver nanoparticles.

Agilent Gene ID	Entrez Gene Name	Gene product (mammalian)	Fold change
A_15_P735641	angiotensin I converting enzyme (peptidyl-dipeptidase A) 1	*ACE*	-0.979
A_15_P720576	aquaporin 9	*AQP9*	-0.460
A_15_P433820	basic helix-loop-helix family, member e41	*BHLHE41*	-0.945
A_15_P111782	CD36 molecule (thrombospondin receptor)	*CD36*	-0.655
A_15_P118478	cell division cycle associated 7	*CDCA7*	-0.682
A_15_P105520	cryptochrome 2 (photolyase-like)	*CRY2*	-1.125
A_15_P112968	E74-like factor 3(ets domain transcrip. factor, epithelial-specif.)	*ELF3*	-0.635
A_15_P193916	G protein-coupled receptor kinase 7	*GRK7*	-0.856
A_15_P688556	guanylate cyclase activator 1C	*GUCA1C*	-0.984
A_15_P664406	heterogeneous nuclear ribonucleoprotein H1 (H)	*HNRNPH1*	0.488
A_15_P667826	low density lipoprotein receptor-related protein 1	*LRP1*	0.420
A_15_P151491	minichromosome maintenance complex component 2	*MCM2*	0.451
A_15_P184201	meprin A, alpha (PABA peptide hydrolase)	*MEP1A*	-0.509
A_15_P759761	NPC1 (Niemann-Pick disease, type C1, gene)-like 1	*NPC1L1*	-0.552
A_15_P110290	nuclear receptor subfamily 1, group D, member 1	*NR1D1*	-1.247
A_15_P160041	nucleoporin 50kDa	*NUP50*	0.417
A_15_P188606	nucleoredoxin-like 1	*NXNL1*	0.351
A_15_P119429	opsin 1 (cone pigments), long-wave-sensitive	*OPN1LW*	1.793
A_15_P103795	orthodenticle homeobox 2	*OTX2*	0.512
A_15_P104502	period homolog 1 (Drosophila)	*PER1*	-1.153
A_15_P121311	polymerase (RNA) I polypeptide A, 194kDa	*POLR1A*	0.391
A_15_P111652	polymerase (RNA) II (DNA directed) polypeptide D	*POLR2D*	0.573
A_15_P492197	replication factor C (activator 1) 3, 38kDa	*RFC3*	0.395
A_15_P747151	rhodopsin	*RHO*	0.903
A_15_P105466	ribonucleotide reductase M1	*RRM1*	0.733
A_15_P113819	solute carrier family 15 (oligopeptide transporter), member 1	*SLC15A1*	-0.712
A_15_P659881	SUB1 homolog (S. cerevisiae)	*SUB1*	0.587
A_15_P103789	L-threonine dehydrogenase	*TDH*	-0.976
A_15_P166596	thyrotrophic embryonic factor	*TEF*	-0.561
A_15_P100927	transmembrane and coiled-coil domains 1	*TMCO1*	-0.352
A_15_P628481	thioredoxin-related transmembrane protein 3	*TMX3*	-0.676

Cardiovascular disease, genetic disorder, hematological disease, hypersensitivity response and ophthalmic disease were identified by IPA to be associated with the gene expression in the group exposed to silver nanoparticles.

Genetic disorder, ophthalmic disease, gastrointestinal disease and inflammatory disease were identified to be associated with the exposure to silver nitrate.

Table 8. Unique genes affected in the larvae exposed to silver nitrate.

Agilent Gene ID	Entrez Gene Name	Gene product (mammalian)	Fold change
A_15_P142661	Rh family, C glycoprotein	*RHCG*	−0,846
A_15_P401105	synaptic vesicle glycoprotein 2B	*SV2B*	−0,414

3.5.1 Toxicological pathways

IPA identified toxicological pathways most significant for the uploaded genes.

Table 9. Toxicological pathways most associated with genes with most significant fold change in the group exposed to silver nanoparticles. Fisher's p-value gives the significance of the annotated pathway and ratios give the number of total molecules known to be involved in the same pathway.

Pathway	Gene products (mammalian)	p-value	Ratio
LXR/RXR activation	*CD36*	1.01E-01	1/79
Mechanism of gene regulation by peroxisome prolifirators via PPARa	*CD36*	1.85E-01	1/95
PPARa/RXRa activation	*CD36*	2.72E-01	1/170
Cardiac hypertrophy	*ACE*	4.16E-01	1/259

IPA was not able to identify any toxicological pathways to be significant for the gene expression induced in the group exposed to silver nitrate.

3.6 Validation of microarray results by qPCR

Fold changes analyzed by microarrays were compared with fold changes detected by qPCR. The expression levels of three of the tested genes were identified to be significantly different in the exposed groups relative to expression in the control. Pearson's correlation coefficient was estimated to 0.81 ($p<0.01$) for the two techniques.

Table 10. Fold change ratios for 10 target genes (n=6) analyzed by microarrays and relative fold change ratios of the same genes normalized for *β-ACTIN* expression analyzed by qPCR (n=6). Mean expression level of each gene in exposed groups was compared to the expression level in the control by the Student's t-test. Gene names can be found in Table 3.

ID	Gene abbreviations	Microarray		qPCR	
		Fold change	p-value	Fold change	p-value
$AgNO_3$					
A_15_P113394	*ABCA1*	-1.267	0.33	-1.062	0.35
A_15_P666681	*BCAP31*	-1.397	0.46	-1.092	0.03*
A_15_P195261	*BOD1*	1.268	0.16	1.010	0.99
A_15_P120264	*PGD*	1.243	0.35	1.071	0.53
A_15_P621206	*ZHX2*	-3.03	0.44	-1.123	0.10
Ag nano					
A_15_P468060	*ALAS1*	-1.593	0.14	-1.042	0.46
A_15_P114663	*AZIN1*	1.293	0.64	1.197	0.03*
A_15_P682056	*HN1*	-1.443	0.66	1.103	0.18
A_15_P113537	*HSPA4*	1.289	0.39	1.088	0.06
A_15_P620136	*INSIG1*	1.262	0.46	1.326	0.01*

* Significantly different from expression in control

All genes analyzed by qPCR showed the same direction of up- or down-regulation as detected by the microarrays, but the magnitude differed to some degree.

4. Discussion

4.1 Characterization of size and size distribution

Based on results from both methods it appears that some of the primary particles were in the agglomerated state in the stock solution used for spiking of fish water. This initial polydispersity was reflected in the DLS characterization and it seems that there was a greater tendency for the nanoparticles to agglomerate in the highest concentration. Increased particle concentration is known to affect the rate of direct particle-to-particle interactions and result in increased rate and degree of agglomeration (Teeguarden et al. 2007).

The intensity-weighted mean hydrodynamic diameters in Table 4 indicate that all particles were larger than 100 nm. DLS have been reported to be sensitive to the presence of aggregates or dust in samples (Kaszuba et al. 2008; MacCuspie 2011; Römer et al. 2011). It is evident from the figures displaying volume distributions of particle sizes contributing to the relative scattering (Figure 9-13) that there were large particles (or dust) of micrometer size present in all but the sample collected from the fish tank dosed with a nominal concentration of 0.1 mg/L. Based on the fact that the stock solutions were made from ultrapure water filtrated with a final filter of 50 nm it is apparent that these particles stem from the tank water, which is further indicated by the two peaks displayed in the figure for the control group (Figure 9) and is most likely excess feed and debris in the water. It appears from our results that scattering from these other particles become increasingly dominant with decreasing nanoparticle concentration and it is possible that this affected the reported mean hydrodynamic diameter (Table 4).

Assessments of samples from the stock solution identified agglomerated particles even after sonication. It is possible that this is a result from the handling and preparation of samples and TEM images may not be an exact reflection of the size distribution administrated to the exposure tanks.

4.2 Survival

An expected drop in survival was observed in all groups from around 10 dpf, which stabilized around 20 dpf. This is in accordance with previous reporting of a natural attrition rate experienced by zebrafish in this period (Andersen et al. 2003; Powers et al. 2010).

Kaplan-Meier plots (Figure 11) and subsequent survival analysis shows that there was significantly better survival in the group exposed to the highest concentration of silver nanoparticles compared to the other groups. Treatment with silver nanoparticles at a concentration of 0.5 mg/L did also show a trend towards a positive effect on survival. However, this was not statistically significant. These observations are in contrast with previous findings were silver nanoparticles have been observed to induce a dose-dependent increase in mortality of zebrafish embryos (Asharani et al. 2008; Lee et al. 2007). Dose-dependent increase in mortality has also been observed for medaka exposed to the same low levels of silver nanoparticles, and resulted in 100 % mortality at 0.8 mg/L (Wu et al. 2010). Our results indicate that exposure to low concentrations, which is predicted to be likely in the environment, may result in a positive effect on survival of fish larvae.

The photon count rate reported from the DLS characterization indicated more agglomeration in the water sample collected from the same exposure group, and may indicate that agglomerated particles are less available or reactive towards fish, perhaps because of sedimentation. However, we did not observe any significant effects on changes in survival in any of the other groups that can substantiate this. Grey particles were observed on the bottom of all tanks dosed with silver nanoparticles in the present study. Analyses of water samples from tanks in other fish exposure studies have detected that the silver concentrations were lower (Griffitt et al. 2009; Scown et al. 2010), indicating that the larvae in this study might have been exposed to lower concentrations than the nominal concentrations.

Previous studies of the effect of higher concentrations of silver nanoparticles on the survival of zebrafish resulted in an estimated LC_{50} (the concentration at which 50% of the individuals dies) value of 25-50 mg/L for zebrafish embryos (Asharani et al. 2008). Griffith et al. (2009) have estimated a no observed effect concentration (NOEC) on survival of adults to be 1.0 mg/L, which indicate that there is a difference in susceptibility to lethal effects between the embryonic and adult stage of zebrafish. Differences in the route of uptake between the embryonic and adult zebrafish can be a possible reason for these differences. While uptake

over the skin has been observed in zebrafish embryos exposed to silver nanoparticles (Asharani et al. 2008; Yeo & Kang 2008; Yeo & Yoon 2009) uptake over gills and/or through the gastrointestinal tract from the water is suggested to be more important for free-swimming juvenile and adult fish of different species (Handy et al. 2008; Scown et al. 2010; Yeo & Yoon 2009).

The results indicated that zebrafish larvae are not susceptible to lethal effects of low concentrations of silver nanoparticles or silver ions when exposed during larval development (6 dpf – 21 dpf). The low exposure concentration (0.01 mg/L) of $AgNO_3$ resulted in the lowest proportion of surviving larvae, although not significantly lower than in controls ($p=0.16$). The present findings contrast with previous results reporting a significant decrease in survival in the same period (10 dpf – 21 dpf) after exposure to the same concentration of $AgNO_3$ (Powers et al. 2010).

4.3 Growth

There was not observed any significant changes in growth (mean body length) of zebrafish larvae exposed to low concentrations of silver nanoparticles or silver nitrate compared the unexposed larvae on 21 dpf. It may be that this is a result of these larvae being more resistant to adverse effects in it surroundings compared to others that did not survive until 21 dpf. Based on these results it appears that exposures to predicted environmentally low concentrations of silver nanoparticles in this window do not affect the growth of larvae surviving until 21 dpf.

The effect on growth was evaluated by Kruskal-Wallis test. Nonparametric methods requires great differences in the parameters tested between groups and have a tendency to result in a Type II error (accepting the null hypothesis when there *is* a significant difference) (Paulson 2008). The risk of such a type II error could have been reduced if the length had been measured with a more fine-scaled tool. However, these findings are in accordance with other studies where the effects of silver nanoparticles on body length were found to be insignificant after exposure of Japanese medaka to concentrations in the same low-level range (< 1 mg/L)(Bar-Ilan et al. 2009; Wu et al. 2010).

4.4 Microbiological analysis

The antibacterial effect of silver nanoparticles have been suggested to be a possible explanation for a reported dose-dependent positive effect on body length and weight of juvenile medaka (Wu et al. 2010).

The microbiological investigations showed that water samples from the group experiencing a positive effect on survival actually had the highest number of bacterial colonies, indicating that silver nanoparticles did not improved water quality by reducing the number of microorganisms. However, these assumptions are difficult to substantiate, considering that the differences in the level of microbes between and within treatments could not be compared statistically.

4.5 Changes in gene expression

A much higher number of genes were found to be significantly affected in larvae exposed to nanoparticles compared with silver nitrate. The number of genes that were identified to be unique for the two groups was almost double for the group exposed to nanoparticles compared to silver nitrate (Table 7 and 8), and indicates that nanoparticles induce different responses in the transcriptome of zebrafish larvae compared to silver ions from silver nitrate. This is in accordance with previous studies comparing the transcriptional profiles in small fish models following exposures to silver nanoparticles and silver nitrate (Chae et al. 2009; Griffitt et al. 2009; Griffitt et al. 2008; Laban et al. 2010).

Two genes were found to be in common for both exposures, i.e. glycoprotein 2 (*GP2*) and phosphodiesterase 6H (*PDE6H*), which might result from dissolution of silver nanoparticles and the release of silver ions. We did not measure silver ion concentrations in any of water samples and are not able to exclude the possibility that nanoparticles worked by a silver ion-mediated mode in regards to functions annotated by IPA to involve the expression of these genes that were in common.

4.5.1 Changes in gene expression following exposure to silver nanoparticles

Cardiovascular disease and genetic disorder were identified by IPA to be highly associated with the gene expression profile induced the group exposed to silver nanoparticles. Most of the functions annotated to be involved with cardiovascular disease and genetic disorder in this study appeared to be connected to the gene encoding angiotensin I converting enzyme (*ACE*).

This enzyme is involved in the renin-angiotensin-aldosteron system known to be involved in regulation of blood pressure and associated with the risk for developing cardiovascular disease (Lonn et al. 1994; Yusuf et al. 2000). Silver nanoparticles have been observed to affect the proliferation and angiogenesis of vascular endothelial cells *in vitro* (Gurunathan et al. 2009; Kalishwaralal et al. 2009; Rosas-Hernandez et al. 2009). It has been demonstrated that silver nanoparticles are capable of penetrating the skin and blood vessels of zebrafish larvae and induce effects on cardiogenesis (Yeo & Yoon 2009). Pericardial edema and effects on heart rate and circulation are frequently observed in studies of effects induced by silver nanoparticles on early development of small fish models such as zebrafish, fathead minnow and medaka (Asharani et al. 2008; Bar-Ilan et al. 2009; Laban et al. 2010; Lee et al. 2007; Wu et al. 2010).

Ophthalmic disease was among the top 5 diseases found to be significantly associated with the transcriptional profile induced by nanosilver. Many of the most up- or down-regulated genes identified after exposure to silver nanoparticles are known to encode proteins involved in phototransduction (i.e. *OPN1LW*, *RHO* and *GUAC1C* and *PDE6H*). Interestingly, both cardiac and eye malformation were observed in zebrafish embryos exposed to silver nanoparticles in the same low dose-range as used in this study (Lee et al. 2007). Silver nanoparticles have also been observed to induce eye defects in Japanese medaka during larval development (Wu et al. 2010).

IPA identified all four toxicological pathways to be significantly associated with the expression of *CD36* (thrombospondin receptor) in larvae exposed to a low concentration of silver nanoparticles. *CD36* is expressed in a variety of cell types, including macrophages, endothelium and smooth muscle cells and is involved in uptake of long-chained lipoproteins (Wood et al 2007). The liver X receptor (LXR), retinoid X receptor (RXR) and peroxisome proliferator activated receptor (PPAR α) are all ligand-activated nuclear receptors that induce

transcription of a variety of genes involved in regulation of many physiological processes (Woods et al. 2007). Expression of *CD36* is known to be induced by activation of nuclear receptors such as PPAR and LXR (Chawla et al. 2001), indicating that exposure to silver nanoparticles involves the activation of such nuclear receptors. Considering that these pathways are known to be involved in uptake and efflux of lipids of the artery wall (Chawla et al. 2001; Sui et al. 2011) it seems that silver nanoparticle-induced changes in gene expression can affect cardiovascular health.

Many of the molecules that were identified to be unique for the gene expression following exposure to silver nanoparticles appear to be highly connected in the top molecular network generated by IPA in the analysis of the gene expression of following exposure to silver nanoparticles. This network is included (Figure 18) to demonstrate the relationships.

Several of the genes that were identified to be significantly differently expressed after exposure to silver nanoparticles are involved in the circadian rhythm signaling pathway (i.e. *BHLHE41*, *CRY2*, *NR1D1*, *PER1*), which appears to be connected with both phototransduction (involves *OPN1LW*, *PDE6H*, *RHO*) and cardiovascular disease (associated with *CD36*) (Hayasaka et al. 2010; Nonaka et al. 2001). The diurnal rhythm of several biological processes, including the expression of photoreceptors in the vertebrate eye and cardiovascular function (and disease) have been observed to be associated with changes in the circadian rhythm signaling system (Dalal et al. 2003; Nonaka et al. 2001; Whitmore et al. 1998). *CRY2*, *PER1* and *BHLHE41* are all involved in the negative feedback-loop of the circadian rhythm pathway in both mammals and zebrafish (Cahill 2002). Both silver nanoparticles and nanoparticles of gold have just recently been observed to affect the expression of genes encoding for components involved in the circadian rhythm in rats (Balasubramanian et al. 2010; Minchenko et al. 2011), which may lead to disturbance of the numerous processes regulated by this rhythmic signaling (Cahill 2002; Reppert & Weaver 2001; Yu & Weaver 2011).

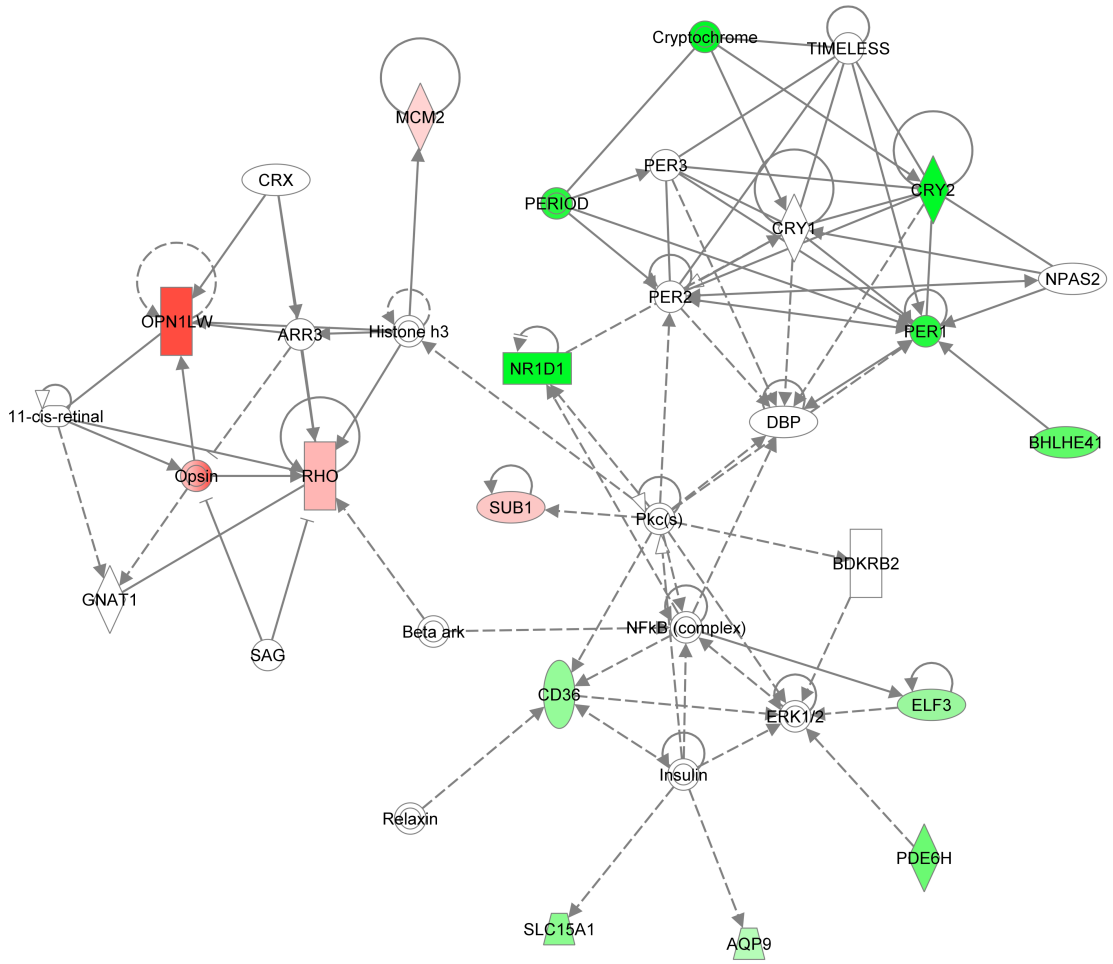

Figure 18. Molecular relationships in the top scored network identified by IPA. The intensity of the node color indicates the degree of up- (red) or down- (green) regulation. Dashed lines means that there is an indirect relationship between the molecules and full lines a direct relationship. All relationships are supported by at least one reference from the information stored in the Ingenuity Knowledge Base.

4.5.2 Gene expression following exposure to silver nitrate

IPA was only able to map 4 gene IDs from the silver nitrate group to objects in the Ingenuity Knowledge Base, which means that few genes were eligible for analysis. Expression of the *GP2* gene was the only gene not identified by IPA to be involved in any of the annotated functions in the analysis, indicating that *PDE6H*, *RHCG* and *SV2B* were more central in regards to effects on gene expression induced by silver ions. Both *RHCG* and *SV2B* are

glycoproteins. Silver has been reported to bind to sulfhydryl and sulphate groups of glycoproteins in epithelia of mussels after accumulation from sea water (George et al. 1986).

The regulation of *PDE6H* in the group exposed to silver nitrate was assigned to function in ophthalmic disease, identified to be a highly significant function associated with the gene expression in the group exposed to silver nanoparticles as well. Coronary artery disease was identified as the toxicological pathway most significantly associated with the gene expression profile following exposure to silver nitrate, and was annotated to the expression of *SV2B*. Synaptic vesicle glycoproteins are involved in transport of neurotransmittors into synaptic vesicles (Feany et al. 1992) and it has just recently been proposed that synaptic vesicle proteins are also significantly expressed in endothelial cells of rat lung microvasculature (Li et al. 2011). Interestingly, have synaptic vesicle proteins just been proposed to be necessary for synaptic transmission in phototransduction (Oberstein et al. 2011), which was identified as significantly associated with the gene expression profiles of both the silver nanoparticle and silver nitrate group. This might indicate that both silver nanoparticles and silver ions induce changes in expression of genes involved in the visual and cardiovascular system, and points towards silver nanoparticles working by a similar mode as silver ions, perhaps through the release of ions at the target site.

It should be noted that a majority of the functions and pathways identified by IPA to be significantly associated to the changes in gene expression have a fairly low ratio in regards to uploaded genes relative to total number of molecules known to be involved in the pathways. Gene expression pathways are complex and may result in other biological outcomes than the ones presented by IPA, which is based on available publications in the Ingenuity Knowledge Base. The literature in the Knowledge Base appears to focus on mammalian research. This bias may be reflected in the observations of IPA annotating cardiovascular disease as most significant for many of the most up- or down-regulated genes, which is a human disease that has gained a lot of attention in the past years.

Quantification of mRNA levels by microarrays can be used to assess the functional state of cells, but do not include translational processes that may modify the level and function of the final proteins (Choi et al. 2010; White & Salamonsen 2005). Microarrays and analyzes of microarray data by applications such as IPA may be useful for designing hypothesis for further testing. By combining microarrays with studies of the proteome and endpoints at

higher organisational levels it may be possible to validate the mapped functions and evaluate the toxicological outcome.

4.6 Validation of microarray results by qPCR

Fold changes of 10 target genes were quantified by qPCR to investigate if the microarray results could be validated by a different quantitative technique. The fold change ratios showed the same direction of regulation, but differed to somewhat in magnitude of up- or down-regulation (Table 10). A Pearson's correlation coefficient of 0.81 indicated that the microarray results correlated well with the results obtained from qPCR.

Selection of genes for validation by qPCR was based on unadjusted p-values <0.05 and means that they were not significant after correction for multiple testing. Three genes were found to be significantly differently expressed in the exposed groups relative to the control based on results from the qPCR, and contrast with the results for the same genes analyzed by microarrays. Real-time qPCR is known to be very sensitive and does not require as much processing of the data as the microarrays, which is evident from these results (White & Salamonsen 2005).

4.7 Ecological relevance

In this study we wanted to evaluate effects of silver nanoparticles at environmentally relevant concentrations. Based on the findings in this study it is implied that silver nanoparticles will not result in adverse effects on survival or growth of fish larvae exposed to concentrations ranging from 0.01 mg/L to 1.0 mg/L in the period they start foraging behavior.

Metallic nanoparticles are expected to agglomerate and sorb to other particles or material in the water due to their high reactivity and raise a question about the bioavailability if released to aquatic environments (Brar et al. 2010; Klaine et al. 2008). It may also be that nanoparticles originating from use, wash or disposal of nanotechnology products will be retained in wastewater treatment plants and pose a bigger risk towards organisms in the soil environment exposed to wastewater sludge containing nanoparticles (Brar et al. 2010).

The present study observed silver nanoparticles to affect the expression level of genes involved in the feedback-loop of the circadian rhythm signaling pathway. *PER1* and *PER2* have been shown to affect the transcriptional activation of *CYP1A1* in mouse exposed to 2,3,7,8-tetrachlorodibenzo-p-dioxin (TCDD) (Qu et al. 2010) and the toxicological pathways annotated to the effects on changes in gene expression in the present study was connected to pathways involving several other ligand-activated nuclear receptors, thus pointing towards an interesting aspect that silver nanoparticles might affect the biotransformation and toxicity of other xenobiotics in the environment.

5. Conclusion

This study was carried out to evaluate the toxicity of silver nanoparticles at predicted environmentally relevant concentrations in a critical window of early life development of zebrafish larvae.

Characterizations of the size and size distributions of the nanoparticles in suspension showed that they were polydispersed and agglomerating even after sonication. Size distributions of silver nanoparticles seem to increase towards bigger diameters with increasing concentrations when dispersed in fish tank water. The mean hydrodynamic diameter characterized by DLS looks to be affected by the presence of bigger particles in the exposure medium.

The results demonstrates a trend towards low concentrations of silver nanoparticles having a positive effect on survival with increasing concentrations, with exposure to 1.0 mg/L resulting in a significant better survival compared to the control. Growth of larvae surviving exposure from 6 dpf – 21 dpf are not affected by low concentrations of silver nanoparticles or silver nitrate (0.01 mg/L).

Exposure to silver nanoparticles (0.01 mg/L) induce significant changes in the expression of a much higher number of genes compared to silver nitrate. Both gene expression profiles appear to associate with the visual system and cardiovascular health. Silver nanoparticles induce changes in several genes involved in the negative feedback-loop of the circadian rhythm system and pathways associated with the activation of nuclear receptors.

Estimated correlation between fold change ratios measured by microarrays and qPCR show that the two methods correlate well in regards to direction of up- or down-regulation and to some degree in magnitude, but qPCR seems to be more sensitive than microarrays in detecting significant differences.

It is indicated from the microbiological analysis of water samples from the fish tanks that the differences in survival appear not be explained by a concentration-dependent antibacterial effect of silver nanoparticles.

Future work

To investigate the size-specific effects and mechanisms of nanoparticles it is suggested that further emphasis should be on studies where the effects of nanoparticles are compared with bigger particles in the micro-meter size.

Cardiovascular disease, phototransduction, processes connected to the expression of the fatty acid translocator (CD36) and circadian rhythm system appear to be associated with the changes in gene expression that were detected in the group exposed to silver nanoparticles (0.01 mg/L). It could be that effects on the gene level will manifest itself on a later stage of development and the significance of disturbances in these functions might be interesting to address in future studies.

Considering that IPA could not map all the genes that were detected to be significantly up- or down regulated to objects in the Ingenuity Knowledge Base it would be interesting to examine which functions or pathways the unmapped genes are involved in.

Dissolution of the nanoparticles and release of silver ions should be quantified.

The microarray results should be validated by qPCR by analyzing 10 genes that are significantly differently expressed based on the adjusted p-values.

References

Ahamed M, AlSalhi MS, Siddiqui MKJ. 2010. Silver nanoparticle applications and human health. *Clinica Chimica Acta* 411:1841-8

Aleström P, Holter JL, Nourizadeh-Lillabadi R. 2006. Zebrafish in functional genomics and aquatic biomedicine. *Trends Biotechnol.* 24:15-21

Andersen L, Holbech H, Gessbo A, Norrgren L, Petersen GI. 2003. Effects of exposure to 17 alpha-ethinylestradiol during early development on sexual differentiation and induction of vitellogenin in zebrafish (Danio rerio). *Comparative Biochemistry and Physiology C-Toxicology & Pharmacology* 134:365-74

Arora S, Jain J, Rajwade JM, Paknikar KM. 2008. Cellular responses induced by silver nanoparticles: In vitro studies. *Toxicology Letters* 179:93-100

Asharani PV, Mun GLK, Hande MP, Valiyaveettil S. 2009. Cytotoxicity and Genotoxicity of Silver Nanoparticles in Human Cells. *ACS Nano* 3:279-90

Asharani PV, Wu YL, Gong ZY, Valiyaveettil S. 2008. Toxicity of silver nanoparticles in zebrafish models. *Nanotechnology* 19

Balasubramanian SK, Jittiwat J, Manikandan J, Ong C-N, Yu LE, Ong W-Y. 2010. Biodistribution of gold nanoparticles and gene expression changes in the liver and spleen after intravenous administration in rats. *Biomaterials* 31:2034-42

Balbus JM, Maynard AD, Colvin VL, Castranova V, Daston GP, et al. 2007. Meeting report: Hazard assessment for nanoparticles - Report from an interdisciplinary workshop. *Environmental Health Perspectives* 115:1654-9

Bar-Ilan O, Albrecht RM, Fako VE, Furgeson DY. 2009. Toxicity Assessments of Multisized Gold and Silver Nanoparticles in Zebrafish Embryos. *Small* 5:1897-910

Bourrachot S, Simon O, Gilbin R. 2008. The effects of waterborne uranium on the hatching success, development, and survival of early life stages of zebrafish (Danio rerio). *Aquatic Toxicology* 90:29-36

Brain JD, Curran MA, Donaghey T, Molina RM. 2009. Biologic responses to nanomaterials depend on exposure, clearance, and material characteristics. *Nanotoxicology* 3:174-80

Brar SK, Verma M, Tyagi RD, Surampalli RY. 2010. Engineered nanoparticles in wastewater and wastewater sludge - Evidence and impacts. *Waste Management* 30:504-20

Braydich-Stolle L, Hussain S, Schlager JJ, Hofmann MC. 2005. In vitro cytotoxicity of nanoparticles in mammalian germline stem cells. *Toxicological Sciences* 88:412-9

Cahill GM. 2002. Clock mechanisms in zebrafish. *Cell and Tissue Research* 309:27-34

Cantor A. 2003. *SAS survival analysis techniques for medical research*. Cary, NC, USA: SAS Pub. viii, 230 s. pp.

Chae YJ, Pham CH, Lee J, Bae E, Yi J, Gu MB. 2009. Evaluation of the toxic impact of silver nanoparticles on Japanese medaka (Oryzias latipes). *Aquatic Toxicology* 94:320-7

Chaloupka K, Malam Y, Seifalian AM. 2010. Nanosilver as a new generation of nanoproduct in biomedical applications. *Trends Biotechnol.* 28:580-8

Chawla A, Boisvert WA, Lee C-H, Laffitte BA, Barak Y, et al. 2001. A PPAR[gamma]-LXR-ABCA1 Pathway in Macrophages Is Involved in Cholesterol Efflux and Atherogenesis. *Molecular Cell* 7:161-71

Choi JE, Kim S, Ahn JH, Youn P, Kang JS, et al. 2010. Induction of oxidative stress and apoptosis by silver nanoparticles in the liver of adult zebrafish. *Aquatic Toxicology* 100:151-9

Cong Y, Banta GT, Selck H, Berhanu D, Valsami-Jones E, Forbes VE. 2011. Toxic effects and bioaccumulation of nano-, micron- and ionic-Ag in the polychaete, Nereis diversicolor. *Aquatic Toxicology* 105:403-11

Croteau MN, Misra SK, Luoma SN, Valsami-Jones E. 2011. Silver Bioaccumulation Dynamics in a Freshwater Invertebrate after Aqueous and Dietary Exposures to Nanosized and Ionic Ag. *Environmental Science & Technology* 45:6600-7

Cumberland SA, Lead JR. 2009. Particle size distributions of silver nanoparticles at environmentally relevant conditions. *Journal of Chromatography A* 1216:9099-105

Dalal JS, Jinks RN, Cacciatore C, Greenberg RM, Battelle BA. 2003. Limulus opsins: Diurnal regulation of expression. *Visual Neuroscience* 20:523-34

DEFRA. 2007. Characterising the potential risks posed by engineered nanoparticles. *Rep. PB12901*, Department for Environment, Food and Rural Affairs, London

Denslow ND, Garcia-Reyero N, Barber DS. 2007. Fish 'n' chips: the use of microarrays for aquatic toxicology. *Mol. Biosyst.* 3:172-7

Dhawan A, Sharma V, Parmar D. 2009. Nanomaterials: A challenge for toxicologists. *Nanotoxicology* 3:1-9

Donaldson K, Stone V, Tran CL, Kreyling W, Borm PJA. 2004. Nanotoxicology. *Occupational and Environmental Medicine* 61:727-8

Dudoit S, Yang YH, Callow MJ, Speed TP. 2002. Statistical methods for identifying differentially expressed genes in replicated cDNA microarray experiments. *Statistica Sinica* 12:111-39

Fako VE, Furgeson DY. 2009. Zebrafish as a correlative and predictive model for assessing biomaterial nanotoxicity. *Advanced Drug Delivery Reviews* 61:478-86

Farkas J, Christian P, Gallego-Urrea JA, Roos N, Hassellöv M, et al. 2011a. Uptake and effects of manufactured silver nanoparticles in rainbow trout (Oncorhynchus mykiss) gill cells. *Aquatic Toxicology* 101:117-25

Farkas J, Christian P, Urrea JAG, Roos N, Hassellov M, et al. 2010. Effects of silver and gold nanoparticles on rainbow trout (Oncorhynchus mykiss) hepatocytes. *Aquatic Toxicology* 96:44-52

Farkas J, Peter H, Christian P, Gallego Urrea JA, Hassellöv M, et al. 2011b. Characterization of the effluent from a nanosilver producing washing machine. *Environment International* 37:1057-62

Faunce T, Watal A. 2010. Nanosilver and global public health: international regulatory issues. *Nanomedicine* 5:617-32

Feany MB, Lee S, Edwards RH, Buckley KM. 1992. The synaptic vesicle protein SV2 is a novel type of transmembrane transporter. *Cell* 70:861-7

Foldbjerg R, Dang DA, Autrup H. 2011. Cytotoxicity and genotoxicity of silver nanoparticles in the human lung cancer cell line, A549. *Arch. Toxicol.* 85:743-50

Forster T, Roy D, Ghazal P. 2003. Experiments using microarray technology: limitations and standard operating procedures. *Journal of Endocrinology* 178:195-204

Fubini B, Ghiazza M, Fenoglio I. 2010. Physico-chemical features of engineered nanoparticles relevant to their toxicity. *Nanotoxicology* 4:347-63

Gaiser BK, Fernandes TF, Jepson M, Lead JR, Tyler CR, Stone V. 2009. Assessing exposure, uptake and toxicity of silver and cerium dioxide nanoparticles from contaminated environments. *Environmental Health* 8

George SG, Pirie BJS, Calabrese A, Nelson DA. 1986. Biochemical and ultrastructural observations of long-term silver accumulation in the mussel, Mytilus edulis. *Marine Environmental Research* 18:255-65

Gottschalk F, Sonderer T, Scholz RW, Nowack B. 2009. Modeled Environmental Concentrations of Engineered Nanomaterials (TiO(2), ZnO, Ag, CNT, Fullerenes) for Different Regions. *Environmental Science & Technology* 43:9216-22

Griffitt RJ, Hyndman K, Denslow ND, Barber DS. 2009. Comparison of Molecular and Histological Changes in Zebrafish Gills Exposed to Metallic Nanoparticles. *Toxicological Sciences* 107:404-15

Griffitt RJ, Luo J, Gao J, Bonzongo JC, Barber DS. 2008. Effects of particle composition and species on toxicity of metallic nanomaterials in aquatic organisms. *Environ. Toxicol. Chem.* 27:1972-8

Gurunathan S, Lee K-J, Kalishwaralal K, Sheikpranbabu S, Vaidyanathan R, Eom SH. 2009. Antiangiogenic properties of silver nanoparticles. *Biomaterials* 30:6341-50

Handy RD, Henry TB, Scown TM, Johnston BD, Tyler CR. 2008. Manufactured nanoparticles: their uptake and effects on fish-a mechanistic analysis. *Ecotoxicology* 17:396-409

Hayasaka N, Larue SI, Green CB. 2010. Differential Contribution of Rod and Cone Circadian Clocks in Driving Retinal Melatonin Rhythms in Xenopus. *Plos One* 5

Hill AJ, Teraoka H, Heideman W, Peterson RE. 2005. Zebrafish as a model vertebrate for investigating chemical toxicity. *Toxicological Sciences* 86:6-19

Hsin YH, Chena CF, Huang S, Shih TS, Lai PS, Chueh PJ. 2008. The apoptotic effect of nanosilver is mediated by a ROS- and JNK-dependent mechanism involving the mitochondrial pathway in NIH3T3 cells. *Toxicology Letters* 179:130-9

Hussain SM, Hess KL, Gearhart JM, Geiss KT, Schlager JJ. 2005. In vitro toxicity of nanoparticles in BRL 3A rat liver cells. *Toxicology in Vitro* 19:975-83

Jones CF, Grainger DW. 2009. In vitro assessments of nanomaterial toxicity. *Advanced Drug Delivery Reviews* 61:438-56

Kalishwaralal K, Banumathi E, Pandian SRK, Deepak V, Muniyandi J, et al. 2009. Silver nanoparticles inhibit VEGF induced cell proliferation and migration in bovine retinal endothelial cells. *Colloids and Surfaces B-Biointerfaces* 73:51-7

Kaszuba M, McKnight D, Connah MT, McNeil-Watson FK, Nobbmann U. 2008. Measuring sub nanometre sizes using dynamic light scattering. *J. Nanopart. Res.* 10:823-9

Kimmel CB, Ballard WW, Kimmel SR, Ullmann B, Schilling TF. 1995. Stages of embryonic development of the zebrafish. *Developmental Dynamics* 203:253-310

Klaine SJ, Alvarez PJJ, Batley GE, Fernandes TF, Handy RD, et al. 2008. Nanomaterials in the environment: Behavior, fate, bioavailability, and effects. *Environ. Toxicol. Chem.* 27:1825-51

Kleinbaum DG, Klein M. 2005. *Survival Analysis: A Self-Learning Text*. New York, NY: Springer Science+Business Media, Inc.

Laban G, Nies LF, Turco RF, Bickham JW, Sepulveda MS. 2010. The effects of silver nanoparticles on fathead minnow (Pimephales promelas) embryos. *Ecotoxicology* 19:185-95

Lee KJ, Nallathamby PD, Browning LM, Osgood CJ, Xu XHN. 2007. In vivo imaging of transport and biocompatibility of single silver nanoparticles in early development of zebrafish embryos. *ACS Nano* 1:133-43

Li Y, Massey K, Witkiewicz H, Schnitzer JE. 2011. Systems analysis of endothelial cell plasma membrane proteome of rat lung microvasculature. *Proteome Science* 9

Liu W, Zhou QF, Liu JY, Fu JJ, Liu SJ, Jiang GB. 2011. Environmental and biological influences on the stability of silver nanoparticles. *Chinese Science Bulletin* 56:2009-15

Livak KJ, Schmittgen TD. 2001. Analysis of relative gene expression data using real-time quantitative PCR and the 2(T)(-Delta Delta C) method. *Methods* 25:402-8

Lonn EM, Yusuf S, Jha P, Montague TJ, Teo KK, et al. 1994. Emerging role of angiotensin-converting enzyme-inhibitors in cardiac and vascular protection. *Circulation* 90:2056-69

MacCuspie RI. 2011. Colloidal stability of silver nanoparticles in biologically relevant conditions. *J. Nanopart. Res.* 13:2893-908

Mahmood M, Casciano DA, Mocan T, Iancu C, Xu Y, et al. 2010. Cytotoxicity and biological effects of functional nanomaterials delivered to various cell lines. *Journal of Applied Toxicology* 30:74-83

Maynard AD, Aitken RJ. 2007. Assessing exposure to airborne nanomaterials: Current abilities and future requirements. *Nanotoxicology* 1:26-41

Maynard AD, Kuempel ED. 2005. Airborne nanostructured particles and occupational health. *J. Nanopart. Res.* 7:587-614

Minchenko DO, Bozhko IV, Zinchenko TO, Yavorovsky OP, Minchenko OH. 2011. Expression of SNF1/AMP-activated protein kinase and casein kinase-1 epsilon in different rat tissues are sensitive markers of in vivo silver nanoparticles action. *Materialwiss. Werkstofftech.* 42:118-22

Morey JS, Ryan JC, Van Dolah FM. 2006. Microarray validation: factors influencing correlation between oligonucleotide microarrays and real-time PCR. *Biological Procedures Online*:175-93

Morones JR, Elechiguerra JL, Camacho A, Holt K, Kouri JB, et al. 2005. The bactericidal effect of silver nanoparticles. *Nanotechnology* 16:2346-53

Mueller NC, Nowack B. 2008. Exposure modeling of engineered nanoparticles in the environment. *Environmental Science & Technology* 42:4447-53

Nel A, Xia T, Madler L, Li N. 2006. Toxic Potential of Materials at the Nanolevel. *Science* 311:622-7

Nonaka H, Emoto N, Ikeda K, Fukuya H, Rohman MS, et al. 2001. Angiotensin II induces circadian gene expression of clock genes in cultured vascular smooth muscle cells. *Circulation* 104:1746-8

Nuber UA. 2005. *DNA microarrays*. Abingdon: Taylor & Francis. XII, 299 s. pp.

Oberdörster G. 2000. Toxicology of Ultrafine Particles: In vivo Studies. *Philosophical Transactions: Mathematical, Physical and Engineering Sciences* 358:2719-40

Oberdörster G, Oberdörster E, Oberdörster J. 2005. Nanotoxicology: An Emerging Discipline Evolving from Studies of Ultrafine Particles. *Environmental Health Perspectives* 113:823-39

Oberdörster G, Sharp Z, Atudorei V, Elder A, Gelein R, et al. 2004. Translocation of inhaled ultrafine particles to the brain. *Inhalation Toxicology* 16:437-45

Oberstein SYL, Lewis GP, Dutra T, Fisher SK. 2011. Evidence that neurites in human epiretinal membranes express melanopsin, calretinin, rod opsin and neurofilament protein. *British Journal of Ophthalmology* 95:266-72

Park E-J, Bae E, Yi J, Kim Y, Choi K, et al. 2010a. Repeated-dose toxicity and inflammatory responses in mice by oral administration of silver nanoparticles. *Environmental Toxicology and Pharmacology* 30:162-8

Park E-J, Yi J, Kim Y, Choi K, Park K. 2010b. Silver nanoparticles induce cytotoxicity by a Trojan-horse type mechanism. *Toxicology in Vitro* 24:872-8

Paulson DS. 2008. *Biostatistics and Microbiology: A Survival Manual*. New York, NY: Springer New York

Powers CM, Yen J, Linney EA, Seidler FJ, Slotkin TA. 2010. Silver exposure in developing zebrafish (Danio rerio): Persistent effects on larval behavior and survival. *Neurotoxicol. Teratol.* 32:391-7

Powers KW, Palazuelos M, Moudgil BM, Roberts SM. 2007. Characterization of the size, shape, and state of dispersion of nanoparticles for toxicological studies. *Nanotoxicology* 1:42-51

Qu X, Metz RP, Porter WW, Neuendorff N, Earnest BJ, Earnest DJ. 2010. The clock genes period 1 and period 2 mediate diurnal rhythms in dioxin-induced Cyp1A1 expression in the mouse mammary gland and liver. *Toxicology Letters* 196:28-32

Reppert SM, Weaver DR. 2001. Molecular analysis of mammalian circadian rhythms. *Annu. Rev. Physiol.* 63:647-76

Rosas-Hernandez H, Jimenez-Badillo S, Martinez-Cuevas PP, Gracia-Espino E, Terrones H, et al. 2009. Effects of 45-nm silver nanoparticles on coronary endothelial cells and isolated rat aortic rings. *Toxicology Letters* 191:305-13

Römer I, White TA, Baalousha M, Chipman K, Viant MR, Lead JR. 2011. Aggregation and dispersion of silver nanoparticles in exposure media for aquatic toxicity tests. *Journal of Chromatography A* 1218:4226-33

Sayes CM, Reed KL, Subramoney S, Abrams L, Warheit DB. 2009. Can in vitro assays substitute for in vivo studies in assessing the pulmonary hazards of fine and nanoscale materials? *J. Nanopart. Res.* 11:421-31

Schrand AM, Braydich-Stolle LK, Schlager JJ, Dai L, Hussain SM. 2008. Can silver nanoparticles be useful as potential biological labels? *Nanotechnology* 19

Scown TM, Santos EM, Johnston BD, Gaiser B, Baalousha M, et al. 2010. Effects of Aqueous Exposure to Silver Nanoparticles of Different Sizes in Rainbow Trout. *Toxicological Sciences* 115:521-34

Skebo JE, Grabinski CM, Schrand AM, Schlager JJ, Hussain SM. 2007. Assessment of metal nanoparticle agglomeration, uptake, and interaction using high-illuminating system. *International Journal of Toxicology* 26:135-41

Smyth GK. 2004. Linear models and empirical bayes methods for assessing differential expression in microarray experiments. *Statistical Applications in Genetics and Molecular Biology* 3

Smyth GK. 2005. *Limma: Linear models for microarray data*. 397-420 pp.

Smyth GK, Speed T. 2003. Normalization of cDNA microarray data. *Methods* 31:265-73

Stebounova LV, Adamcakova-Dodd A, Kim JS, Park H, O'Shaughnessy PT, et al. 2011. Nanosilver induces minimal lung toxicity or inflammation in a subacute murine inhalation model. *Particle and Fibre Toxicology* 8

Sui YP, Xu JX, Rios-Pilier J, Zhou CC. 2011. Deficiency of PXR decreases atherosclerosis in apoE-deficient mice. *J. Lipid Res.* 52:1652-9

Takenaka S, Karg E, Roth C, Schulz H, Ziesenis A, et al. 2001. Pulmonary and systemic distribution of inhaled ultrafine silver particles in rats. *Environmental Health Perspectives* 109:547-51

Tang J, Xiong L, Wang S, Wang J, Liu L, et al. 2008. Influence of silver nanoparticles on neurons and blood-brain barrier via subcutaneous injection in rats. *Applied Surface Science* 255:502-4

Teeguarden JG, Hinderliter PM, Orr G, Thrall BD, Pounds JG. 2007. Particokinetics in vitro: Dosimetry considerations for in vitro nanoparticle toxicity assessments. *Toxicological Sciences* 95:300-12

Tiede K, Boxall ABA, Tear SP, Lewis J, David H, Hassellov M. 2008. Detection and characterization of engineered nanoparticles in food and the environment. *Food Additives and Contaminants* 25:795-821

Trickler WJ, Lantz SM, Murdock RC, Schrand AM, Robinson BL, et al. 2010. Silver Nanoparticle Induced Blood-Brain Barrier Inflammation and Increased Permeability

in Primary Rat Brain Microvessel Endothelial Cells. *Toxicological Sciences* 118:160-70

Wei L, Tang J, Zhang Z, Chen Y, Zhou G, Xi T. 2010. Investigation of the cytotoxicity mechanism of silver nanoparticles in vitro. *Biomedical Materials* 5

Westerfield M. 2000. *The zebrafish book: a guide for the laboratory use of zebrafish (Danio rerio)*. [Eugene, OR]: M. Westerfield. 1 bind (Flere pag.) pp.

Wettenhall JM, Smyth GK. 2004. limmaGUI: A graphical user interface for linear modeling of microarray data. *Bioinformatics* 20:3705-6

White CA, Salamonsen LA. 2005. A guide to issues in microarray analysis: application to endometrial biology. *Reproduction* 130:1-13

Whitmore D, Foulkes NS, Strahle U, Sassone-Corsi P. 1998. Zebrafish Clock rhythmic expression reveals independent peripheral circadian oscillators. *Nat. Neurosci.* 1:701-7

Wijnhoven SWP, Peijnenburg WJGM, Herberts CA, Hagens WI, Oomen AG, et al. 2009. Nano-silver - a review of available data and knowledge gaps in human and environmental risk assessment. *Nanotoxicology* 3:109 - 38

Woods CG, Heuvel JPV, Rusyn I. 2007. Genomic profiling in nuclear receptor-mediated toxicity. *Toxicologic Pathology* 35:474-94

Wu YA, Zhou QF, Li HC, Liu W, Wang T, Jiang GB. 2010. Effects of silver nanoparticles on the development and histopathology biomarkers of Japanese medaka (Oryzias latipes) using the partial-life test. *Aquatic Toxicology* 100:160-7

Yeo MK, Kang M. 2008. Effects of nanometer sized silver materials on biological toxicity during zebrafish embryogenesis. *Bulletin of the Korean Chemical Society* 29:1179-84

Yeo MK, Yoon JW. 2009. Comparison of the Effects of Nano-silver Antibacterial Coatings and Silver Ions on Zebrafish Embryogenesis. *Molecular & Cellular Toxicology* 5:23-31

Yu EA, Weaver DR. 2011. Disrupting the circadian clock: Gene-specific effects on aging, cancer, and other phenotypes. *Aging-Us* 3:479-93

Yusuf S, Sleight P, Pogue J, Bosch J, Davies R, et al. 2000. Effects of an angiotensin-converting-enzyme inhibitor, ramipril, on cardiovascular events in high-risk patients. *New England Journal of Medicine* 342:145-53

Zhang C, Willett C, Fremgen T. 2003. Zebrafish: An Animal Model for Toxicological Studies. In *Current Protocols in Toxicology*: John Wiley & Sons, Inc.

Appendix A: DLS characterization conditioned water

Results from the DLS characterization of a sample of the conditioned water, which was used for diluting the stock solutions to required nominal concentrations.

Table A.1. Mean hydrodynamic diameter, polydispersity index (PDI) and photon count rate (thousand counts per second) of particles detected in the conditioned water.

Sample	Z.avg (d.nm)	PDI	Count rate (kcps)
Conditioned water	484	0,40	157

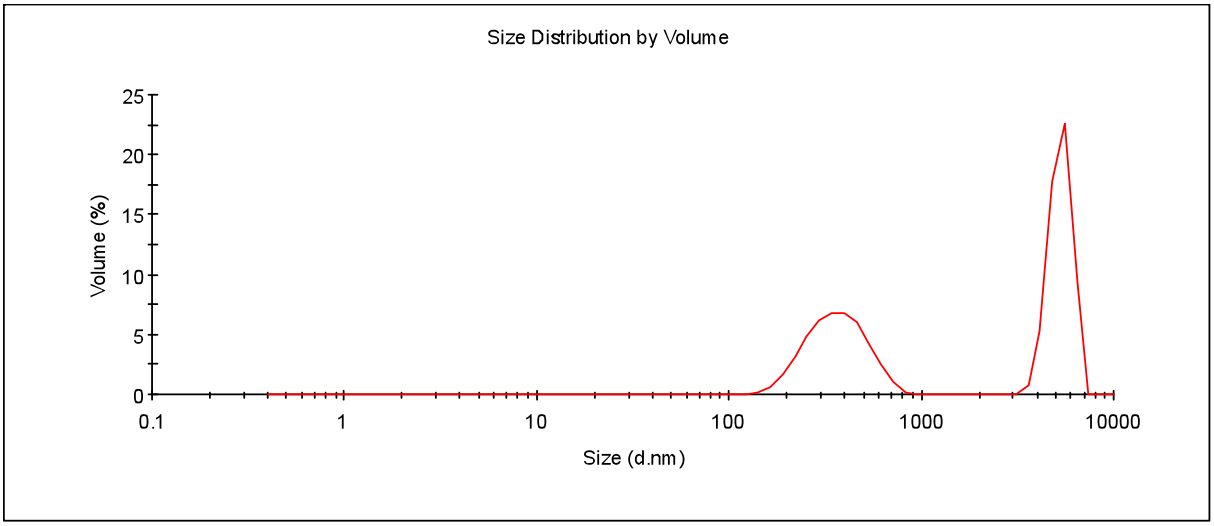

Figure A.1. Volume distributions of relative light scattered by populations of particles in various size classes in the sample collected from the conditioned water used for dillutions of the stock solutions. The y-axis is the relative intensity of scattered light and particle size is presented on a logarithmic x-axis.

Mean size of the particles contributing to the two peaks displayed in Figure A.1 were reported to be 379 nm and 5305 nm for the left and right peaks respectively.

Appendix B: Raw data survival

Table B.1. Number of surviving larvae recorded on a daily basis from 6 dpf – 13 dpf. Raw data from 14 dpf – 21 dpf can be found in table B.2.

Group	Conc. (mg/L)	Rep	6 dpf	7 dpf	8 dpf	9 dpf	10 dpf	11 dpf	12 dpf	13 dpf
Control	0	A	52	52	52	52	51	49	41	38
Control	0	B	52	52	52	52	52	49	40	37
Control	0	C	52	52	52	52	51	46	43	36
Control	0	D	52	52	52	52	52	48	40	35
Control	0	E	52	52	51	51	49	47	41	35
AgNO3	0,01	A	52	52	52	52	52	48	41	34
AgNO3	0,01	B	52	52	51	51	48	44	37	34
AgNO3	0,01	C	52	52	52	52	49	46	35	32
AgNO3	0,01	D	52	52	52	52	49	47	34	27
AgNO3	0,01	E	52	52	52	52	52	50	45	45
Ag nano	0,01	A	52	50	50	50	50	49	45	33
Ag nano	0,01	B	52	52	52	52	51	47	40	39
Ag nano	0,01	C	52	52	52	52	50	45	41	36
Ag nano	0,01	D	52	52	52	51	50	41	35	33
Ag nano	0,01	E	52	51	51	51	50	47	43	38
Ag nano	0,1	A	52	52	52	52	52	47	40	35
Ag nano	0,1	B	52	52	52	52	48	44	38	36
Ag nano	0,1	C	52	52	51	51	51	46	34	32
Ag nano	0,1	D	52	52	52	52	51	48	41	35
Ag nano	0,1	E	52	52	52	51	51	47	42	38
Ag nano	0,5	A	52	52	52	51	51	49	41	40
Ag nano	0,5	B	52	52	52	51	51	47	39	34
Ag nano	0,5	C	52	52	52	51	50	45	39	37
Ag nano	0,5	D	52	52	52	50	50	45	41	41
Ag nano	0,5	E	52	52	51	50	50	47	44	40
Ag nano	1	A	52	52	52	52	51	47	46	44
Ag nano	1	B	52	52	52	52	52	50	46	44
Ag nano	1	C	52	52	52	52	50	48	47	44
Ag nano	1	D	52	51	51	51	51	49	46	45
Ag nano	1	E	52	51	51	51	50	49	49	46

Table B.2. Number of surviving larvae recorded on a daily basis from 14 dpf – 21 dpf.

14 dpf	15 dpf	16 dpf	17 dpf	18 dpf	19 dpf	20 dpf	21 dpf
35	35	35	35	34	33	32	30
35	35	35	35	34	34	34	32
35	35	34	34	34	34	32	32
33	31	31	31	31	31	31	31
34	34	33	33	32	32	32	31
33	33	31	31	31	31	30	30
34	32	31	27	26	26	26	26
28	25	25	25	25	25	25	24
26	24	24	23	23	23	23	23
42	41	41	41	41	41	41	41
32	31	31	30	30	28	28	28
38	36	35	35	34	34	34	34
36	35	35	35	34	34	34	34
31	31	30	29	29	28	28	27
37	36	36	35	35	35	35	35
34	34	33	33	33	33	33	33
36	35	35	34	34	34	32	32
31	31	31	30	30	30	29	28
34	31	30	30	30	29	28	25
37	37	35	34	32	31	31	30
40	40	40	38	38	38	37	36
34	34	33	33	33	33	30	30
36	35	35	35	35	35	35	35
41	39	39	38	38	38	38	37
40	40	40	40	40	39	39	38
39	39	39	39	39	39	39	38
44	43	41	39	39	39	39	39
42	41	39	39	38	38	38	37
44	42	40	40	39	39	39	39
46	45	45	43	41	41	41	41

Appendix C: Length data

Length of each larvae surviving until 21 dpf was measured and mean length in each tank was used as observational unit.

Table C.1. Mean length in each replicate tank on 21 dpf.

Group	Replicate tank	n	Mean	Std.dev
Control	A	25	0,472	0,041
Control	B	32	0,477	0,042
Control	C	28	0,488	0,049
Control	D	30	0,495	0,060
Control	E	30	0,500	0,061
AgNO3 0.01	A	28	0,476	0,049
AgNO3 0.01	B	26	0,474	0,051
AgNO3 0.01	C	23	0,485	0,043
AgNO3 0.01	D	21	0,466	0,052
AgNO3 0.01	E	33	0,472	0,051
Ag nano 0.01	A	27	0,482	0,063
Ag nano 0.01	B	32	0,497	0,059
Ag nano 0.01	C	28	0,490	0,063
Ag nano 0.01	D	26	0,504	0,054
Ag nano 0.01	E	32	0,490	0,047
Ag nano 0.1	A	31	0,489	0,067
Ag nano 0.1	B	30	0,497	0,058
Ag nano 0.1	C	22	0,496	0,042
Ag nano 0.1	D	25	0,488	0,038
Ag nano 0.1	E	26	0,502	0,053
Ag nano 0.5	A	33	0,494	0,060
Ag nano 0.5	B	28	0,503	0,055
Ag nano 0.5	C	32	0,502	0,046
Ag nano 0.5	D	34	0,471	0,060
Ag nano 0.5	E	34	0,477	0,059
Ag nano 1.0	A	33	0,493	0,071
Ag nano 1.0	B	34	0,487	0,057
Ag nano 1.0	C	34	0,481	0,064
Ag nano 1.0	D	34	0,480	0,052
Ag nano 1.0	E	35	0,476	0,058

Appendix D: Microarray results Ag nano

Top tables (Table D.1 and Table D.2) with raw data displaying the significantly differently expressed genes identified following exposure to silver nanoparticles. Genes with log expression values (logFC) in-between -0.3 and 0.3 and average expression (AveExpr) under 0.6 were excluded from the dataset.

Table D.1. Significantly differently expressed genes identified in the group exposed to silver nanoparticles (0.01 mg/L). Expression values (log FC), average expression (AveExpr) and significance based on p-values adjusted for multiple testing assigned by limmaGUI.

Name	ID	GeneName	logFC	AveExpr	adj,P,Val
ENSDART00000043507	A_15_P111207	si:ch211-284a13,1	-1,10699248	6,83754629	0,00052007
NM_131577	A_15_P101039	arntl1a	1,02701244	6,69358944	0,00089664
NM_205729	A_15_P110290	nr1d1	-1,24710023	7,64409873	0,00136078
ENSDART00000043507	A_15_P177056	si:ch211-284a13,1	-0,87237631	7,04376232	0,0035406
NM_131253	A_15_P117046	opn1mw1	0,97498916	8,174265	0,0035406
NM_212439	A_15_P104502	per1b	-1,15297452	8,16143591	0,00416137
NM_194393	A_15_P688556	guca1c	-0,98363909	7,70345935	0,00547377
NM_001031841	A_15_P193916	grk7a	-0,85553169	8,24474915	0,00547377
NM_131400	A_15_P166596	tef	-0,56059336	6,966742	0,00689295
NM_201580	A_15_P160041	nup50	0,41652026	7,46160186	0,00689295
NM_200692	A_15_P196411	ndrg1l	0,59211677	6,43636707	0,00689295
NM_131786	A_15_P161566	cry3	-1,25801662	8,46270214	0,00738407
TC396958	A_15_P753176		-1,27722289	7,43328583	0,00763601
ENSDART00000114637	A_15_P403295	wu:fb81h03	-0,71296628	6,36433596	0,00763601
NM_198064	A_15_P113819	slc15a1b	-0,71219696	8,18463277	0,00763601
NM_131788	A_15_P103946	cry5	-0,46623726	6,86524969	0,00763601
NM_001076637	A_15_P118404	zgc:153034	0,53242536	7,30402384	0,00763601
TC417879	A_15_P670036		-0,66401333	7,24811718	0,00764198
BC044335	A_15_P133416	dnmt1	0,50907404	6,5524634	0,00764198
NM_199972	A_15_P116591	elovl4b	0,5281247	7,00006294	0,00764198
ENSDART00000060098	A_15_P399665		0,70845868	7,46649326	0,00764198
EH438071	A_15_P513272	wu:fc15e02	-0,86021259	8,23956184	0,00808831
NM_001159826	A_15_P404370	zgc:112320	-0,89681929	6,67810001	0,01090137
NM_001002443	A_15_P119429	opn1lw2	1,79323705	8,16885304	0,01244836
TC403556	A_15_P759761		-0,55192622	6,99794178	0,01317382
NP13322337	A_15_P760451		-0,49891234	6,76020902	0,01396086
ENSDART00000058699	A_15_P397660	LOC557984	-0,35567774	6,08922191	0,01396086
BC096780	A_15_P263411	cry2b	0,71735068	6,84903972	0,01435172
NM_001025188	A_15_P196306	zgc:110409	-0,55640454	6,67268753	0,0169118

Top table generated from the microarrays for the group exposed to silver nanoparticles is continued below.

Table D.2. Significantly differently expressed genes identified in the group exposed to silver nanoparticles (0.01 mg/L). Expression values (log FC), average expression (AveExpr) and significance based on p-values adjusted for multiple testing assigned by limmaGUI.

Name	ID	GeneName	logFC	AveExpr	adj,P,Val
NM_212637	A_15_P206111	mat2a	-0,888807	8,32666673	0,01812927
BC131854	A_15_P433820	bhlhb3l	-0,94501184	6,90377511	0,02171458
TC396958	A_15_P406095		-1,09082049	7,16238986	0,02285693
ENSDART00000114501	A_15_P121311		-0,39147835	7,60031947	0,02390181
CN322620	A_15_P554197		-0,59683605	6,10032449	0,02487935
NM_001003598	A_15_P108422	nutf2	0,49189273	7,69581907	0,02487935
TC391195	A_15_P112968		-0,63500327	8,2778159	0,02514456
NM_001110760	A_15_P188606	nxnl1	0,35068263	6,32386585	0,02514456
NM_001017574	A_15_P118478	zgc:110113	0,68205537	7,22266914	0,02514456
NM_201457	A_15_P492197	rfc3	0,39469487	6,18706192	0,02709214
NM_001033096	A_15_P720576	aqp9a	-0,45972239	7,07600862	0,02785881
CK015579	A_15_P772801	wu:fj84d10	-1,14689024	7,86856063	0,03156172
NM_001109843	A_15_P666946	rhcgl1	-0,70826515	7,3554759	0,03197057
NM_212589	A_15_P664406	hnrnph1l	0,48825044	7,65685433	0,03197057
NM_131084	A_15_P213761	rho	0,77963347	11,2197711	0,03376626
NM_001002575	A_15_P100927	tmco1	-0,35220868	7,15893122	0,03547341
NM_131251	A_15_P103795	otx2	0,51203874	6,77910395	0,03547341
BC125850	A_15_P177836		0,80747898	7,67617658	0,03547341
TC388547	A_15_P735641		-0,97880223	6,59542861	0,03861332
NM_001004618	A_15_P648216	zgc:103408	-0,3920372	8,25207287	0,03861332
NM_173257	A_15_P151491	mcm2	0,45128834	8,16876209	0,03861332
NM_001017803	A_15_P765676	zgc:111983	-0,74057985	8,29824929	0,04025804
TC451970	A_15_P672296		-0,58965221	7,00836332	0,04150678
TC388466	A_15_P678566		-0,46933043	6,47556659	0,04150678
NM_001002317	A_15_P111652	polr2d	0,5734794	7,77580343	0,04150678
NM_131455	A_15_P105466	rrm1	0,73271486	7,82232072	0,04150678
NM_213245	A_15_P103789	tdh	-0,97569941	8,71755423	0,04476046
TC391598	A_15_P600272		-0,53770367	7,02320649	0,04476046
BC044385	A_15_P118042	cry4	0,58411484	6,1908332	0,04476046
BC165490	A_15_P659881	zgc:109973	0,58665359	7,36452006	0,04476046
NM_001020557	A_15_P628481	tmx3	0,67561474	6,10455035	0,04476046
NM_001128727	A_15_P184201	mep1a,2	-0,5092089	7,48768393	0,04650052
BC093428	A_15_P770971	kif5a	0,54481471	8,24013659	0,04650052
NM_001002363	A_15_P111782	cd36	-0,65515324	8,93708454	0,04733669
ENSDART00000038471	A_15_P667826		0,4197346	6,81152107	0,04733669
NM_131253	A_15_P153321	opn1mw1	1,21518898	8,38043916	0,04847486

Appendix E: Microarray results $AgNO_3$

Top table of raw data displaying the significantly differently expressed genes identified following exposure to silver nitrate. Genes with log expression values (logFC) in-between -0.3 and 0.3 and average expression (AveExpr) under 0.6 were excluded from the dataset.

Table E.1. Significantly differently expressed genes identified in the group exposed to silver nitrate (0.01 mg/L). Expression values (log FC), average expression (AveExpr) and significance based on p-values adjusted for multiple testing assigned by limmaGUI.

Name	ID	GeneName	logFC	AveExpr	adj,P,Val
NM_001159826	A_15_P404370	zgc:112320	-1,37498073	6,73677338	0,00109251
NP13322337	A_15_P760451		-0,51957119	6,80499295	0,00214754
NM_001082995	A_15_P401105	zgc:158677	-0,4140721	6,23068911	0,00295127
NM_001089577	A_15_P142661	zgc:162132	-0,84644983	6,62590681	0,01569884
EH550393	A_15_P378415		-0,70598627	7,77639999	0,01807794
NM_212756	A_15_P151571	grn2	-0,61305622	8,97274013	0,02440055
	A_15_P764346		-0,54247123	6,81119017	0,03484891

Appendix F: Raw data qPCR

Raw data and calculations involved in the qPCR analysis are presented below.

Table F.1. Amplification efficiencies calculated from the C_T values and slopes of the standard curves generated from the 10 fold dilution of all primers. The percent efficiency is calculated by taking (E-1) times 100%. And an ideal reaction has E near 2.

Gene	Slope ctrl	*E control*	*Slope exp*	*E exposed*	*Mean*
ABCA1	2.872	2.229	2.9994	2.155	2.192
ALAS1	3.3114	2.004	3.2327	2.039	2.022
AZIN1	3.6176	1.89	3.4576	1.946	1.918
BCAP31	3.323	2	3.2391	2.036	2.018
BOD1	3.4009	1.968	3.1258	2.089	2.028
HN1	3.1711	2.067	2.793	2.281	2.174
HSPA4	3.3311	1.996	3.3271	1.998	1.997
INSIG1	3.1574	2.074	3.3393	1.993	2.033
PGD	3.5196	1.924	3.5579	1.91	1.917
ZHX2	3.1317	2.086	3.1844	2.061	2.073
BACT	3.253	2.03	3.2401	2.035	2.032